

## Mitigation of methane emissions from Vietnamese local cattle (Lai Sind) by cashew nut shell liquid (CNSL) feeding

Livestock production, especially ruminant production, is known to be one of the most significant sources of greenhouse gas (GHG) emissions in Southeast Asian countries. Therefore, there is an urgent need to develop technologies to mitigate GHG emissions from this sector in the region. A significant amount of cashew nuts is produced in Vietnam, leaving a significant amount of cashew shells as by-product. Cashew nut shell liquid (CNSL), extracted from the cashew shell, is known to contain antimicrobial compounds like anacardic acid, which can inhibit the activity of methanogens in the rumen of ruminants. Here, we evaluated the effect of CNSL feeding on methane emission from local cattle (named Lai Sind) in Vietnam. We also revealed the effect of CNSL on the activity of the microbiome in the rumen and its function, thus paving the way for the development of an effective CNSL feeding technology for GHG mitigation.

Lai Sind cattle, the most widespread cattle breed in Vietnam, were used for the CNSL feeding experiment ( $n=4$ ), with an average body weight of  $246.1\pm 22.6$  kg for Run 1 and  $375.0\pm 36.0$  kg for Run 2. The amounts of CNSL fed were 4 and 6 g/100 kg body weight per day for Runs 1 and 2, respectively.

Average methane emission per kg dry matter intake was reduced from 20.2% to 23.4% by CNSL feeding (Figs. 1A and 1B). Furthermore, CNSL feeding had a significant effect on the  $\delta^{13}\text{C}$  value of the methane produced, indicating that it significantly affected organic matter degradation in the rumen (Fig. 1C). CNSL feeding also affected the relative proportion of propionate in the short-chain fatty acid concentration in the rumen (Run 1: 8.2%  $\rightarrow$  10.6%,  $p=0.001$ ; Run 2: 17.7%  $\rightarrow$  21.4%,  $p=0.015$ ), while it did not affect feed degradation efficiency (data not shown). CNSL feeding significantly reduced the relative abundance of a major methanogen (order *Methanobacteriales*) while it significantly increased the relative abundance of family *Prevotellaceae*, which is known to degrade the polysaccharide or produce propionate (Fig. 2A). The estimated function of the rumen microbiome indicates that CNSL feeding significantly suppressed methane metabolism, which agrees with methane emission measurement, and that it enhanced carbohydrate metabolism or lipid metabolism at the same time (Fig. 2B). The results of 16S rRNA gene amplicon sequencing suggest that CNSL significantly reduced the diversity of the rumen microbiome, and the results of network analysis further indicate that a major methanogen (order *Methanobacteriales*) changed the functional partner in the rumen with the significant metabolic relationship (Fig. 2C).

(K. Maeda, T. Suzuki [National Agriculture and Food Research Organization (NARO)], V.T. Nguyen, V.P. Le, M.C. Nguyen [Can Tho University, Vietnam], K. Yamada, K. Kudo, N. Yoshida [Tokyo Institute of Technology], C. Hikita [Idemitsu Kosan. Co. Ltd.]

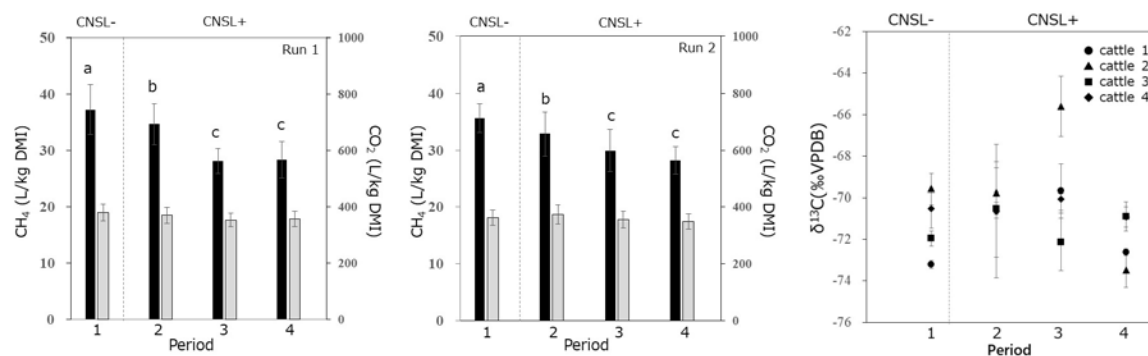


**Fig. 1. Enteric CH<sub>4</sub> (black) and CO<sub>2</sub> (grey) emissions per kg dry matter intake (DMI) from Lai Sind cattle, with (periods 2–4) and without (period 1) CNSL feeding (n = 4)** Error bars: standard deviation (SD). Different letters indicate significant differences (*P* < 0.05). Different doses of CNSL were set in Run 1 (4 g/100 kg BW: A) and Run 2 (6 g/100 kg BW: B). C. Changes in the  $\delta^{13}\text{C}$  values of enteric CH<sub>4</sub> (Run 1). The  $\delta^{13}\text{C}$  values are expressed as relative to the VPDB (Vienna Pee Dee Belemnite). Each symbol (circle, triangle, square, and diamond) indicates individual cattle. Error bar: SD (n = 3)

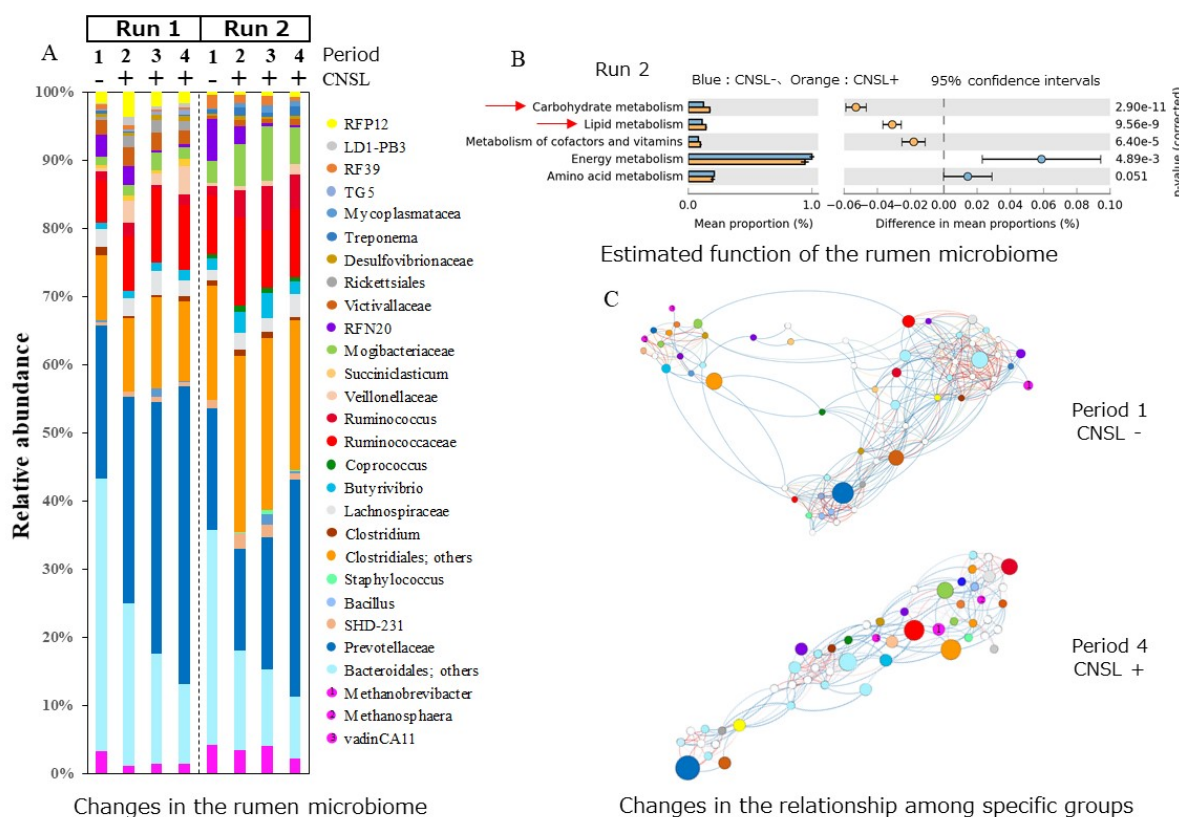


**Fig. 2. Effect of CNSL feeding on rumen microbiome** A. The effect of CNSL feeding on relative abundance of each group of the bacteria/archaea. B. Estimated function of the rumen microbiome and significantly changed features by CNSL feeding in Run 2. Orange and light blue at the bottom of the dendrogram indicate the results with (periods 2–4) and without (period 1) CNSL feeding. C. Output of network analysis for period 1 (without CNSL feeding) and period 4 (with CNSL feeding)

## Potential mitigation of life cycle greenhouse gas emissions from rice cultivation by alternate wetting and drying (AWD)

Alternate wetting and drying (AWD) has been introduced in Vietnam's Mekong delta to reduce soil methane (CH<sub>4</sub>) emissions from rice (*Oryza sativa* L.) cultivation, to mitigate climate change, and to save water consumption. The benefits of AWD (e.g., reducing irrigation cost and increasing yields) have been reported by many researchers, including researchers in Japan International Research Center for Agricultural Sciences and Can Tho University. However, there is less information about the trade-off among soil CH<sub>4</sub> emissions reduction, nitrous oxide (N<sub>2</sub>O) emissions, and agronomic management. The present study carried out a life cycle assessment to evaluate the impacts of AWD on potential mitigation of life-cycle greenhouse gas (LC-GHG) emissions.

A structured interview was carried out in An Giang Province, Vietnam, which is the 5th-largest rice producer in the world. In August and September 2019, 200 farmers were interviewed: 100 farmers with 199 fields and 100 non-AWD farmers with 187 fields. Vietnamese staff members of Can Tho University conducted the interviews. The system boundary and functional unit for the LCA were defined as a cradle-to-farm gate and 1 ha of paddy rice, respectively. The soil and non-soil CH<sub>4</sub> and N<sub>2</sub>O emissions for the AWD and non-AWD farmers were estimated with reference to the IPCC tier 1 methodology (2019). The present study showed that AWD farmers lowered the use of seeds, nitrogen, phosphate fertilizers, and operation hours of irrigation pumps without decreasing rice yields. Despite an increase in N<sub>2</sub>O emissions by 17% due to wet (anaerobic) - dry (aerobic) cycles by AWD which enhances nitrification-denitrification processes, and application rates of potassium, LC-GHG emissions were reduced by 41%, lowering soil CH<sub>4</sub> emissions by 47% and non-soil GHG emissions (burning straw and other managements) by 9%. LC-GHG emissions from AWD farmers and non-AWD farmers were estimated to be 9.82 and 16.6 t CO<sub>2</sub>-eq ha<sup>-1</sup>, respectively. Unlike water management, straw management had little influence on the CH<sub>4</sub> emissions difference between groups, as >75% of farmers irrespective of the water management carried out on-site burning as straw management. To the best of the authors' knowledge, the present study is one of the first studies to survey rice straw management under different water management strategies.

These results can be utilized as scientific evidence for policy making and implementation. In addition, they can be used to estimate potential mitigation of LC-GHG emissions for a country where AWD is introduced. Moreover, the methodology used in the present study can be applied for the other countries.

A. Leon, K. Minamikawa, T. Izumi, N.H. Chiem [Can Tho University])

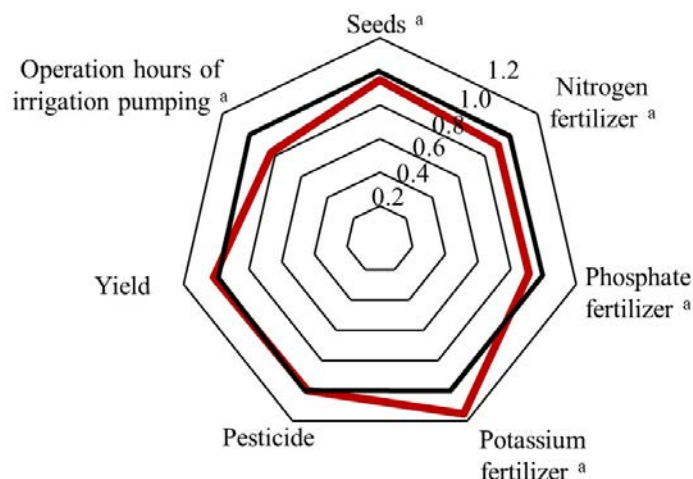


**Fig. 1. Ratios of AWD farmers to non-AWD farmers in the use of seeds, nitrogen, phosphate, potassium fertilizers, pesticide, yield, and operation hours of irrigation pumping**

The red line in the chart shows the ratio of AWD farmers to non-AWD farmers. If the ratio is greater than 1, the value of the corresponding item for AWD farmers is greater than that of non-AWD farmers (a: Significantly different at  $p < 0.05$ ).

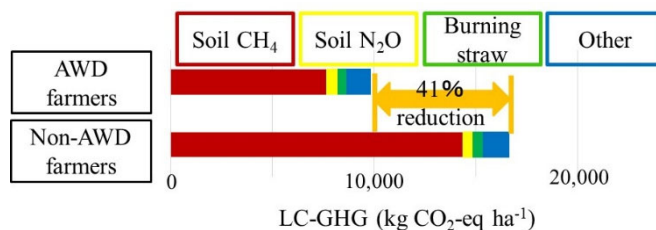


**Fig. 2. Comparing GHG emissions between AWD farmers and non-AWD farmers**

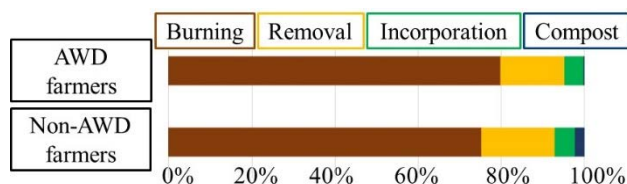


**Fig. 3. Rice straw management between AWD farmers and non-AWD farmers**

### **Monitoring saline intrusion in the Ayeyarwady Delta, Myanmar, using satellite data**

Myanmar's agricultural sector, which contributes to most of the country's gross domestic product has great potential. After the government supported the installation of irrigation facilities in 1992, the double cropping system became widespread in Myanmar, and rice production and population both increased in the well-irrigated lowlands of the Ayeyarwady Delta. However, despite the presence of irrigation facilities, rice cropping is impractical near the coast because irrigation water is severely affected by high salinity during the dry season, limiting crop growth and rendering the soil unsuitable for many crops. Therefore, saline intrusion is one of the biggest factors limiting crop production in the Ayeyarwady Delta.

Previous studies based on remote sensing have related the optical variables of water color, such as salinity, turbidity, and suspended sediment concentrations, to single spectral bands. These empirical models are often region- and time-dependent and thus should be calibrated and validated with data that cover a wide range of field conditions. This means that models need to be developed for specific water bodies or sensors. The aims of this study therefore are to (1) develop empirical models by fitting field measurements from three rivers (i.e., the Patheingyi, Ywè and Pyawbwe Rivers) and two sampling occasions (i.e., beginning and end of the dry season) to Sentinel-2 imagery, (2) monitor the spatial and temporal variability of saline intrusion in the Ayeyarwady Delta during the dry season, and (3) assess the impact of saline intrusion on the distribution patterns of paddy fields.

The imagery of Sentinel-2 was suitable for monitoring saline intrusion because of its high spatial (10-m) and temporal (10-day) resolutions. We found that the reflectance of the visible bands correlated with electrical conductivity (EC), which in turn was influenced by the concentration and composition of dissolved salts. When the river water mixed with salt water from the sea, suspended particles tended to flocculate and settle, indicating that less turbid water was more saline. The best-fitting model was obtained with the green band (coefficient of determination  $R^2$  of 0.78, root mean square error of 4.90 dS m<sup>-1</sup>, and mean absolute error of 3.34 dS m<sup>-1</sup>). The saline intrusion, which showed considerable spatial and temporal variability during the dry season, extended approximately 80 km inland at the end of the dry season in March at Patheingyi River. The 1 ppt salt concentration line in March marked the boundary between cultivated and non-cultivated areas of the paddy field, indicating that cultivable areas were strongly affected by saline intrusion. The results show that more frequent monitoring and use of higher resolution Sentinel-2 image data can support effective water resource management.

*(T. Sakai, K. Omori, A. N. Oo [Yezin Agricultural University], Y. N. Zaw [Department of Agriculture, Myanmar])*

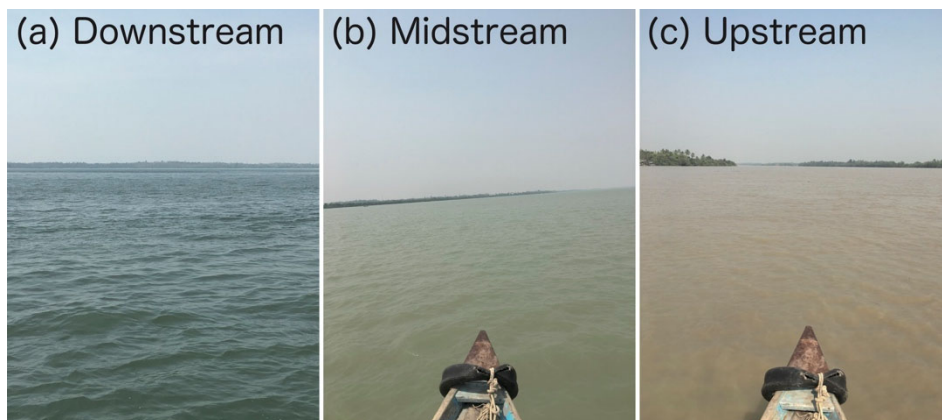


**Fig. 1. Photographs of river water conditions in the (a) downstream, (b) midstream, and (c) upstream reaches of Ywe River on 9 March 2018**

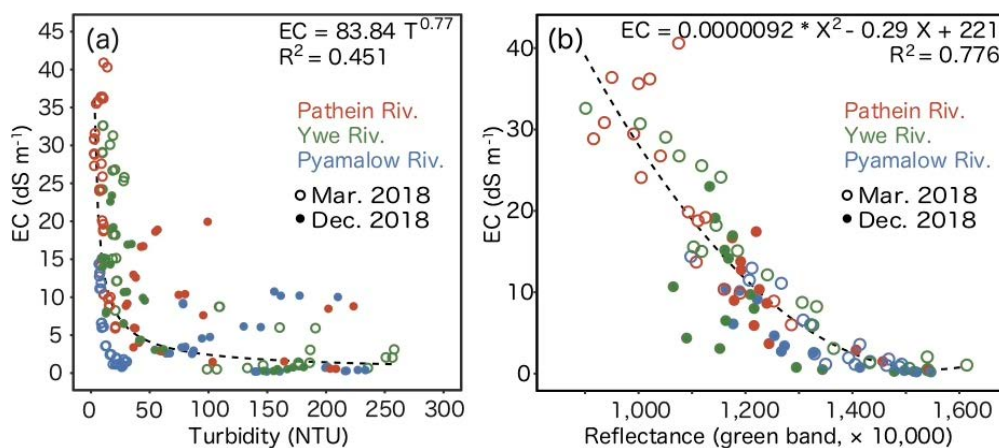


**Fig. 2. Relationships between (a) turbidity and electrical conductivity (EC), and (b) EC and green band reflectance retrieved from Sentinel-2**

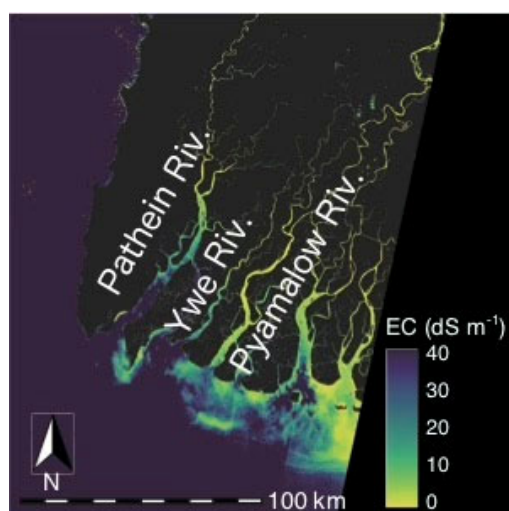


**Fig. 3. Spatial distribution of EC on 12 March 2018**

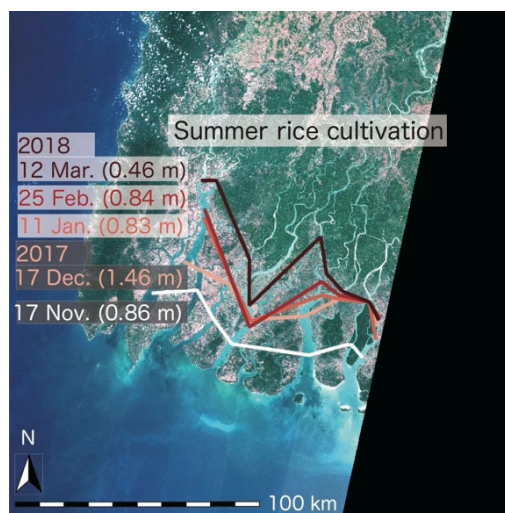


**Fig. 4. The 1 ppt salt concentration lines during the dry season**

The lines connect locations where EC is  $1.56 dS m^{-1}$  (i.e., 1 ppt).

## **Soil oxidation conditions during the initial growth period of ratoons could contribute to improve the yield performance of ratoons**

Compared with conventional double-season rice cropping, ratoon rice cropping can reduce production cost because of its advantages in labor, seed, seedbed and water savings. However, the grain yield of ratoon rice is only 40%–60% that of the main crop; thus, most of ratoon cropping is only practiced by farmers as an afterthought. In recent years, in West Sumatra, Indonesia, a perennial rice cropping system called SALIBU has been practiced and found to produce a yield equivalent to that of single rice cropping multiple times annually. Therefore, this study focused on the SALIBU method, whose unique features are double-cutting of stem and humid soil moisture management during the harvesting stage (Fig. 1), in order to find the factors that increase the yield of ratoon. We conducted cultivation trials using a concrete tank (Fig. 2) in Naypyidaw, Myanmar, to evaluate the effect of the cutting times and the soil moisture regimes on grain yield and regeneration rate of ratoon in tropical regions.

Experiments were conducted using a concrete tank filled with paddy to evaluate cutting regimes (single- and double-cutting) and soil moisture regimes (saturated, moist and dry). Double cropping (main crop + 1<sup>st</sup> ratoon) was carried out from February to August 2019 (first trial), and triple cropping (main crop + 2<sup>nd</sup> ratoon + 3<sup>rd</sup> ratoon) was implemented from September 2019 to May 2020 (second trial). Summarizing for the moisture regimes, the soil water potentials of the saturated, saturated-moist, moist, and dry regimes were approximately 0 kPa, –5 kPa, –11 kPa, and –19 kPa, respectively, and the soil redox potentials of the saturated, saturated-moist, moist and dry were 200 mV, 100 mV, 200 mV, and 550 mV, respectively. There were significant differences between moisture regimes with regard to grain yield and regeneration rate of tiller (Fig. 3 and Fig. 4). Double cutting (a cutting height of 30–40 cm for harvesting and a height of 5 cm for ratooning) had no positive effect on grain yield and regeneration rate compared with single cutting. If there is no increase in yield commensurate with the cost of the additional cutting, stem cutting of ratoon should be cut once with a height of 5 cm at the time of harvesting. The dried soil moisture conditions promote the increase of easily-decomposable nitrogen compounds and the supply of inorganic nitrogen, and activates root respiration. Hence, improving the rhizosphere environment in the initial growth stage of ratoon in soil under oxidation conditions will contribute toward increasing the yield of ratoon.

The above scenario is the result of using a concrete tank that allows for easy drainage management, and various drainage measures such as designing the drainage channel must be considered to improve the yield of ratoon in paddy fields. Water management (amount, frequency, and period of irrigation) during the harvesting stage of the previous crop should be carried out while considering the air temperature, rainfall, water retention of paddy soil, and plant growth of ratoon.

*(S. Shiraki, K. Yamaoka, Thin Mar Cho [Department of Agricultural Research (DAR), Myanmar], Khin Mar Htay [DAR])*



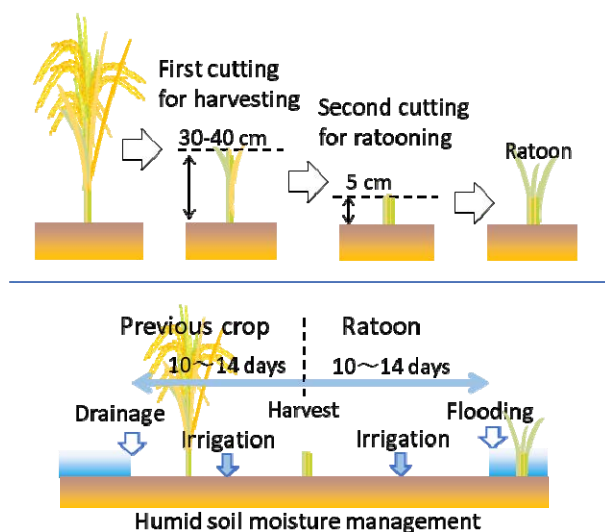


**Fig. 1. Double cutting of stem and soil moisture management during the harvesting stages of the previous crop, which are unique features of Indonesia’s perennial rice cropping system (SALIBU)**



**Fig. 2. Cultivation trial using concrete tanks (L 1.8 m × W 0.9 m × D 0.4 m) in a split-plot design, comprising a total of 24 plots (2 cutting, 3 moisture and 4 replications)**

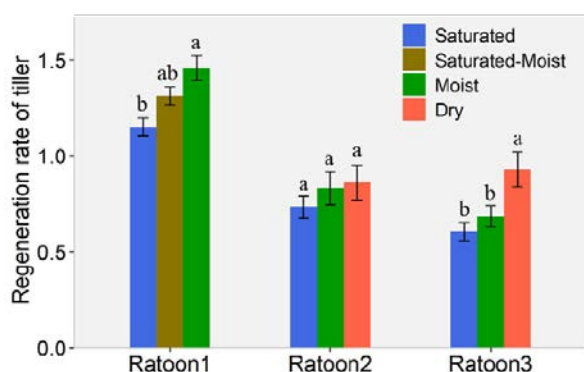


**Fig. 3. Effect of soil moisture regime on the regeneration rate of ratoon crops at 3 weeks after harvesting**

Ratoon crops were harvested by the single cutting of stem. Regeneration rate of tiller was defined as the ratio calculated by the tiller of ratoon divided by that of residual stubble. Error bars indicate the standard errors (n = 16). Same letters above the bar indicate that there is no significant difference at the 5% level by Tukey’s HSD test.

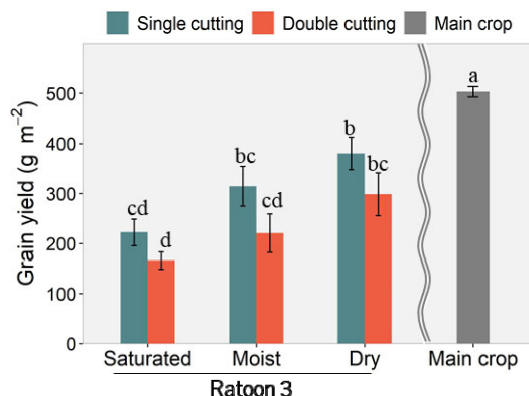


**Fig. 4. Effect of cutting times and soil moisture regimes on the grain yield of ratoon, shown by comparing the 3<sup>rd</sup> ratoon with the main crop**

The error bars indicate the standard errors (n = 4). Same letters above the bar indicate that there is no significant difference at the 5% level by Tukey’s HSD test.



## **Silage preparation improves feed utilization of sorghum and pearl millet stover**

Sorghum (*Sorghum bicolor* [L.] Moench) and pearl millet (*Pennisetum glaucum* L.) are the main crops in the semi-arid region of West Africa. After harvest, the stovers of the two crops are usually exposed and stored outdoors. These stovers are used as roughage for ruminants during dry season when there is a severe shortage of feed. However, the drying of feed resources is the only storage method in this area, and a longer storage time reduces the nutritional value of feed due to leaching and decomposition of nutrients. Therefore, silage prepared using crop stover is expected to alleviate feed shortages in the dry season and improve livestock productivity.

After panicle harvest, the sorghum and pearl millet stovers were exposed in the field and garden for 120 days under natural weather conditions. At the same time, fresh stover silages were prepared using a small-scale fermentation system and stored for 120 days. Compared to fresh stover, both types of stover after 120 days of exposure reduced crude protein and fat content and energy, and increased indigestible crude fiber and lignin. On the other hand, stover silage preparation produced good-quality feed, and the nutrients were not lost after 120 days of ensiling (Fig. 1). Lactic acid bacteria were present in both fresh stovers, but after 120 days of exposure, the counts of harmful microorganisms such as aerobic bacteria, coliform bacteria, yeast, and mold increased, and no lactic acid bacteria were detected. After 120 days of ensiling, lactic acid bacteria became the predominant population and inhibited the growth of harmful microorganisms. As far as the microbial community is concerned, there were no great difference between crop stovers under the same storage treatment (Fig. 2). The prepared silage was of good quality, lactic acid fermentation reduced the pH, and low moisture inhibited butyric acid fermentation. The silage did not deteriorate, and the feed nutrients were well preserved for a long time. Sixteen native beef cattle with an average weight of  $257.4 \pm 13.5$  kg were fed 1 kg of concentrate and free-feeding roughage, including sorghum stover and silage. The intake and feed utilization rate of stover silage significantly ( $p < 0.05$ ) improved compared to exposed stover (Fig. 3).

In terms of utilization of results, farmers in the semi-arid areas of West Africa can easily use local crop stover resources for silage, reducing the shortage of feed for ruminants in the dry season. The silage preparation technology will be released as a technical report by the CNRST (Burkina Faso National Center for Scientific Research and Technology) to improve local livestock raising method. Fresh sorghum and pearl millet stovers after harvest usually have low moisture, so when preparing silage, the moisture should be adjusted to about 60%.

(Y. Cai, S. Yamasaki, D. Jethro [Institute of Environment and Agricultural Research (INERA)], M. Nignan [INERA])

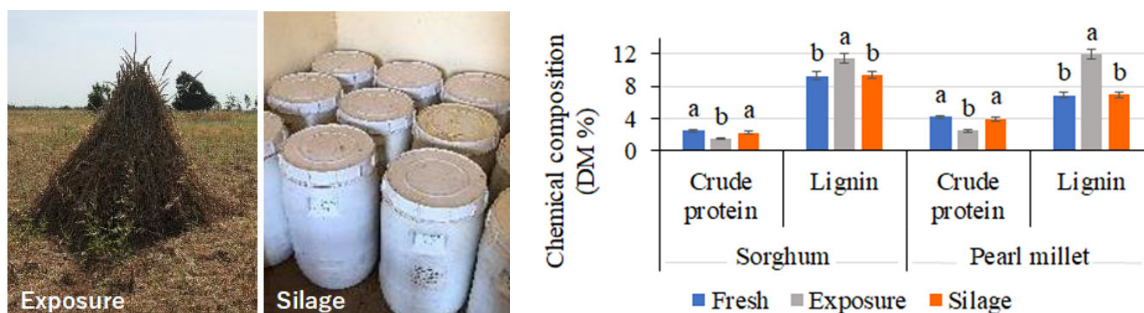


**Fig. 1. Storage of crop stovers during exposure and ensiling (left) and changes in their chemical composition (right)**

<sup>a, b</sup> Means of three samples differ significantly ( $p < 0.05$ ).

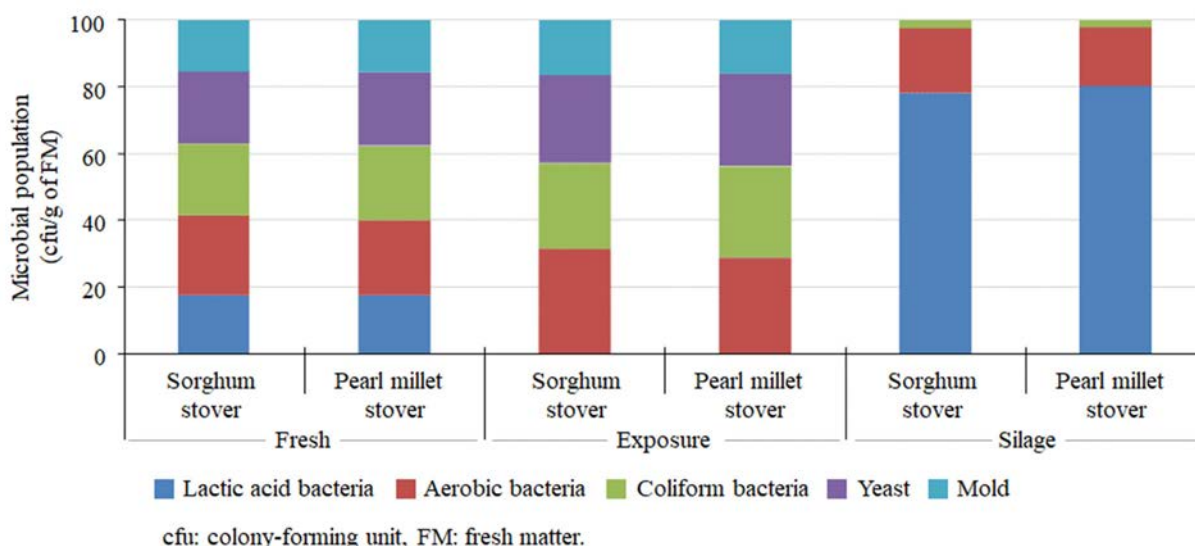


**Fig. 2. Microbial population due to differences in the preservation method of crop stover**

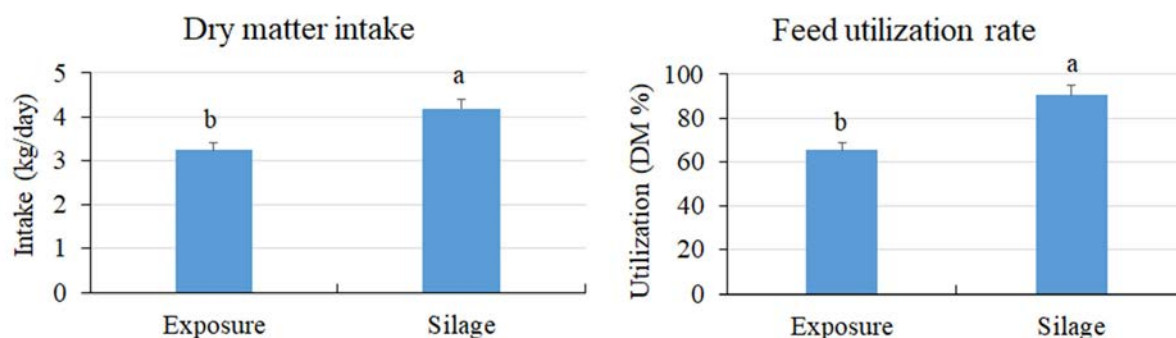


**Fig. 3. Dry matter intake and feed utilization rate of beef cattle due to differences in storage method of sorghum stover**

Feed utilization rate = cattle intake / total feed × 100%.

<sup>a, b</sup> Means of eight cattle differ significantly ( $p < 0.05$ ).

## **Providing information on collaborative behaviors is important for communal forest management in Ethiopia**

Many forests in northern Ethiopian highlands are communal forests managed by local farmers. These farmers collectively adopt soil and water conservation practices, such as construction of stone bunds and excavation of deep trenches, to maintain forests and supervise reforestation (Fig. 1). All members of a rural community are supposed to engage in the conservation without cash payment, in exchange for them being able to collect animal fodder and firewood. However, there are concerns over the longevity of the collaboration.

The sustainability of communal forests depends on whether or not local people are aware of the importance of collaboration in conservation activities. This study investigates whether providing information regarding the importance of collaboration in conservation work using an economic experiment approach enhances farmers' cooperative behavior in Ethiopia.

We conducted an economic experiment called the "public goods game" for participants randomly selected from eleven villages in Tigray Region, Ethiopia. Each session involved ten rounds of the game. The procedure of the experiment followed the standard public goods game. Each participant was asked to contribute any amount worth up to 5 ETB (Ethiopian Birr) for communal forest conservation. During the initial instruction, we explained the rules of the experiment and consequences of the investment. Also, just after the 5th round of each game, we repeated the instruction, same as that offered before starting the game. The result shows that while the average contribution continues to decline until the 5th round, it jumps up at the 6th round to almost the same level as the 1st round (Fig. 2). The speed of the decline after the 6th round is slower than that before the 5th round (Table 1). These results suggest that repeating the instruction has a positive impact on local people's collaboration. Moreover, we have found heterogeneity in the contribution in terms of social and household characteristics (Table 2). Also, the contribution is higher if other members contribute a larger amount in the previous round (Table 2). This demonstrates endogeneity in voluntary contributions.

The results of this study suggest that conducting periodic seminars to remind local farmers of the benefits of communal land could enable them to maintain a high level of commitment to natural resource conservation and sustainable development. It should be noted, however, that farmers' collaboration for natural resource management may vary among countries, ethnic groups, and geographic characteristics.

*(S. Oniki, H. Etsay [Mekelle University], M. Berhe [Mekelle University], T. Negash [Mekelle University])*



**Fig. 1. A soil and water conservation structure for reforestation built through farmers' community work**

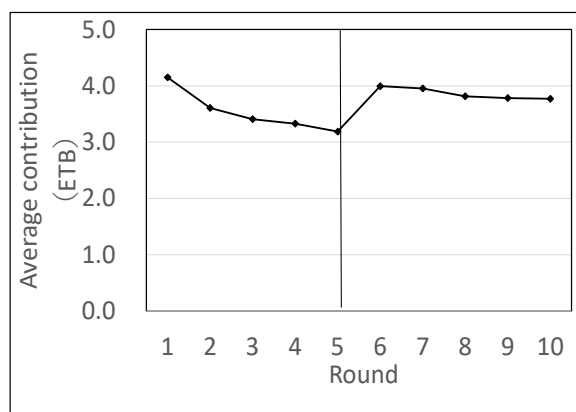


**Fig. 2. Average contribution by round**  
The vertical line indicates the timing of intervention.

**Table 1. Changes in average contribution from Rounds 1 to 5, 5 to 6, and 6 to 10 (ETB)**

Period	Round 1 to 5	Round 5 to 6	Round 6 to 10
Change in contribution	-0.963***	0.808***	-0.224***
Difference from Round 1-5	-	1.771***	0.739***

Note: Average of all participants. \*\*\* $p < 0.01$ .

**Table 2. Determinants of contribution in the public goods game: Tobit regression model**

Variable	Coefficient estimate	Variable	Coefficient estimate
Contribution of other members	1.084***	Distance from town	0.021***
Female	-0.09	Trust among villagers	0.395***
Education	0.014	Farmland area	-0.112**
Age	0.206***	Animal holding	-0.008
Soil fertility	-0.213***		

Note: Contribution of other members: the average value of the contribution in the previous round for all of the other participants (ETB: Ethiopian Birr). Female: female participant. Education: a length of formal education (years). Age: Age of participant. Soil fertility: the dummy variable for soil type (0 if Calcisols is dominant and 1 otherwise). Distance from town: distance from a district center to home (km). Trust among villagers: dummy variable to indicate whether villagers trust each other or not. Farmland area: size of participants' farmland area (ha). Animal holding: the number of livestock in the tropical livestock unit. \*\*\* $p < 0.01$ , \*\* $p < 0.05$ .

## **Modified conservation agriculture for taro production in combination with spot excavation by gas-powered apparatus and organic mulch**

Taro (*Colocasia esculenta* (L.) Schott) is traditionally produced as a main staple crop in a coastal swamp of the Pacific islands. Sea level rise due to climate change, however, often causes saltwater to intrude into the taro fields and push the taro production area up toward inland slopes. Soils in the volcanic upland of the Pacific islands, however, are heavily weathered and acidic and are extremely infertile with a shallow surface organic layer. Thus, soil fertility should be improved in order to enhance taro production without soil erosion and disturbance to corals which, incidentally, attract many foreign tourists. Conservation agriculture (CA), a farming method composed of three principles, namely, minimum soil disturbance, permanent residue cover, and diverse rotations, is suggested to be the best management practice for improving nutrient cycles and soil organic matter restoration and controlling soil erosion. In this study, the effects of tillage and mulching on soil erosion and upland taro production were investigated, with modifications to the three CA principles depending on applicability to local farmers and availability of local resources.

The experiment was conducted from August to May at a research station in Palau Community College in Babeldaob Island, Republic of Palau. The slopes of the experimental plots were between 8 to 13 degrees, while the total rainfall was 2,800 mm during the cropping season. We introduced a gas-powered portable auger or a self-propelled trencher as a modified technology for minimum tillage and for planting (Fig. 1). After excavating the soil with these apparatuses down to 45 cm depth, the excavated soil and 300 g of compost were mixed and returned into the hole/ditch up to 25 cm depth. Taro seedlings (cultivar: Ngesaus etc.) were then planted in the hole or ditch. As modifications of permanent residue cover and diverse rotations, we tested three types of mulch (yard long beans/sweet potato living mulch, and betel nut leaf mulch) in combination with modified minimum tillage.

When taro was cultivated in combination with modified minimum tillage and local organic mulch (betel nut leaf), taro yield increased by 3.2 to 3.6 times (1.8 to 2.0 t ha<sup>-1</sup>) compared to control (full tillage without mulch) (Fig. 2). When the portable auger was used, a single corm weighed heavier by 2.6 times (256 g per fresh corm) compared to control. In addition, the combination of modified minimum tillage and organic mulch decreased soil erosion by 80% to 91% (from 35 m<sup>3</sup> ha<sup>-1</sup> to 3.1–6.9 m<sup>3</sup> ha<sup>-1</sup>) (Fig. 3).

In conclusion, minimum tillage using a portable auger with betel nut leaf mulch can be recommended as a modified CA method for upland taro production specially in the Republic of Palau where extremely infertile steep inland areas are expected to be developed.

(H. Omae, Y.Y. Nwe [Palau Community College])



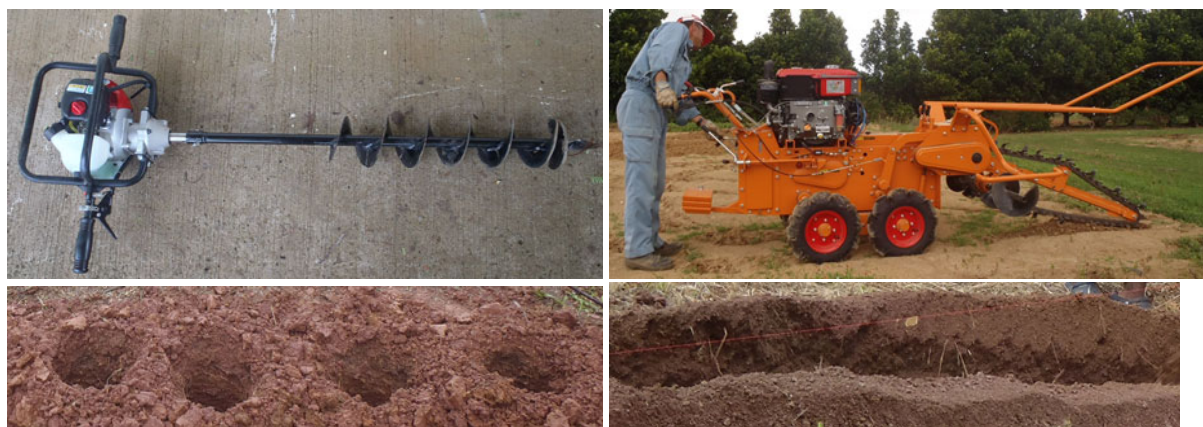


**Fig. 1. Gas-powered portable auger (left) and self-propelled trencher (right)**

Left: Gas-powered portable auger (AGZ5010EZ, ZENNOH, Japan) attached with a drill (15 cm in diameter, 80 cm in length); Right: Self-propelled trencher (NF-827-II, KAWABE, Japan)

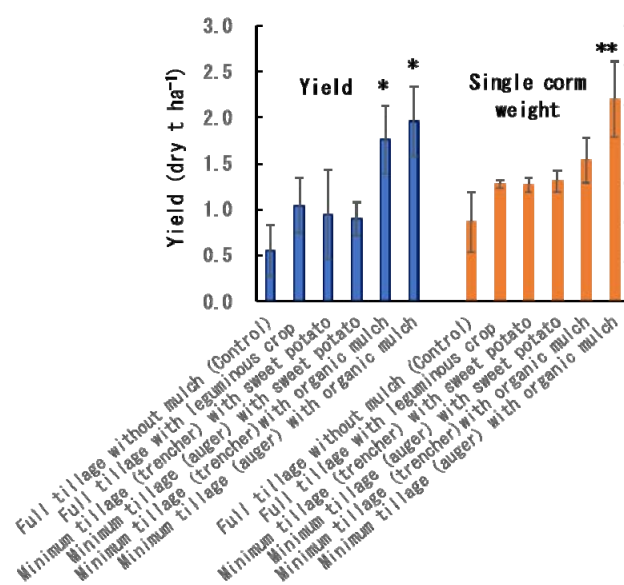


**Fig. 2. Combination effects of modified minimum tillage and surface mulch on taro yield and single corm weight**

\*, \*\*: Significantly different from control

(\* :  $p < 0.05$ , \*\* :  $p < 0.01$ ) (Dunnett's test)

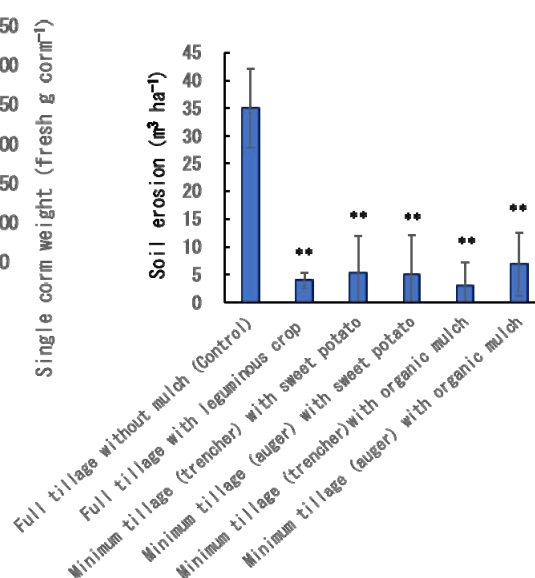


**Fig. 3. Combination effects of modified minimum tillage and surface mulch on soil erosion**

To measure eroded soil, experimental plot was enclosed with a wooden frame and soil trap was installed at the down end.

\*\*: Significantly different from control

(\*\* :  $p < 0.01$ ) (Dunnett's test)



## **Nitrogen leaching and growth of sugarcane under different nitrogen fertilization levels in a subtropical island**

In tropical and subtropical islands where highly permeable limestone rocks are distributed, rainfall causes nitrogen (N) from chemical fertilizers to readily leach underground, with the nitrate leached from fertilization of sugarcane becoming a main source of groundwater pollution. The effect of excessive amounts of fertilizer in early growth stage of sugarcane, before the development of the root system, is limited. Therefore, it is important that fertilizer management should be appropriate for the growth characteristics of sugarcane. This study aimed to develop a fertilizer application technique that reduces N load to groundwater while maintaining sugarcane yield by using a drainage lysimeter.

Our research site was the Japan International Research Center for Agricultural Sciences, Tropical Agricultural Research Front (JIRCAS-TARF), located in Ishigaki Island, Japan. Drainage lysimeters with an area of 10 m<sup>2</sup> and a depth of 2 m were filled with dark red soil derived from limestone, and sugarcane was planted without irrigation (Fig. 1). Drainage water was collected at the bottom of lysimeters and the concentration of nitrate nitrogen (NO<sub>3</sub>-N) in drainage water was measured using a spectrophotometer. The experimental design consisted of a randomized block with two replications of a 3 × 2 factorial design and an unfertilized control, totaling 14 plots. The first factor was the N rates of the basal applications (0, 35, or 70 kg N ha<sup>-1</sup>) and the second factor was the N rates of the supplementary applications (80 or 160 kg N ha<sup>-1</sup>) (Table 1). Even when the basal N was reduced to 50% of the current fertilizer application standard (T2), the same level of yield was maintained as in T1 where 100% basal N was applied. The timing of fertilizer application is important because T4 with halved N in the supplemental fertilizer has higher yield than T3 with no basal fertilizer, even though the total amount of N applied is lower. Concentrations of NO<sub>3</sub>-N in drainage water were high in the early growth stage period from late April to late June, and high concentrations of 8 to 10 mg L<sup>-1</sup> were detected in the conventional fertilizer rate (T1) (Fig. 2). In the supplemental N-only 50% (T4), basal N 50% (T2 and T5), and basal N 0 application (T3 and T6) plots, the accumulated N leaching was reduced by 10 kg ha<sup>-1</sup>, 12 kg ha<sup>-1</sup>, and 19 kg ha<sup>-1</sup>, respectively, compared to the current fertilizer application of 24 kg ha<sup>-1</sup> (T1) (Fig. 3). Even if the amount of N applied under the current fertilizer application is reduced by 15% (equivalent to 35 kg ha<sup>-1</sup>), N leaching from fertilizer could be reduced by about 50% (12 kg ha<sup>-1</sup>) while maintaining the same level of sugarcane yield.

The results of this study will provide basic data for the revision of the standard fertilization (amount of fertilizer applied) for sugarcane cultivation in Okinawa Prefecture, as well as information for the analysis of N balance and dynamics in the groundwater basin. For appropriate fertilizer management, it is necessary to consider the surrounding environmental conditions in addition to reducing the amount of nitrogen. Therefore, accumulating soil and meteorological data and using them for model analysis is effective.

*(K. Okamoto, T. Anzai, S. Ando, S. Goto [National Agriculture and Food Research Organization Kyushu Okinawa Agricultural Research Center])*

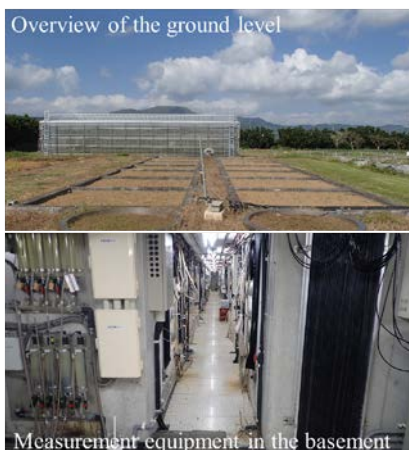


**Fig. 1. Drainage lysimeters at JIRCAS-TARF**

**Table 1. Sugarcane yield and leaf area in each N treatment**

No.	Treatments		Harvest survey			Growth survey	
	Basal N (kg ha <sup>-1</sup> )	Supplementary N (kg ha <sup>-1</sup> )	Cane yield per plot (t ha <sup>-1</sup> )	Cane yield per stalk (kg)	Stalk density (stalks m <sup>-2</sup> )	Leaf area in April (cm <sup>2</sup> )	Leaf area in August (cm <sup>2</sup> )
T1	70	160	91.0	1.13 a	8.4 a	83.3 a	295 a
T2	35	160	88.8	1.11 a	7.9 a	84.5 a	275 a
T3	0	160	76.8	1.03 a	8.4 a	87.4 a	272 a
T4	70	80	83.0	1.01 a	8.4 a	98.3 a	270 a
T5	35	80	74.5	1.07 a	6.8 a	86.3 a	250 ab
T6	0	80	72.3	1.06 a	7.1 a	82.3 a	241 b
T7	0	0	39.8	0.75 b	7.9 a	91.3 a	215 b

Note 1: Treatments (T1–T7) refer to different N application rates.

Note 2: There is a significant difference between different alphabets among N treatments by Tukey method ( $p < 0.05$ ).

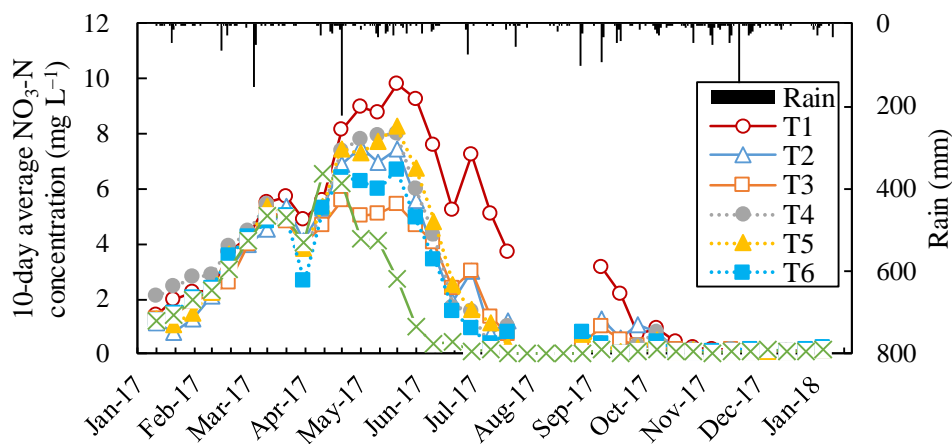


**Fig. 2. NO<sub>3</sub>-N concentration in drainage water**

Note: Treatments (T1–T7) refer to different N application rates.

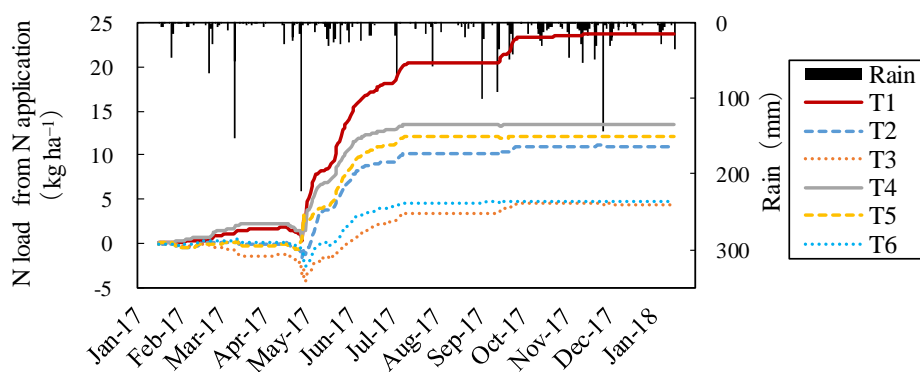


**Fig. 3. N load from N application**

Note 1: Treatments (T1–T7) refer to different N application rates.

Note 2: N load from N application refers to the accumulated N loads in T1 to T6 minus that in T7 (control treatment).

## **Brachiaria reduces nitrification rate through inhibition of Ammonia-oxidizing archaea in inter-plant soil**

Modern agriculture requires large amounts of nitrogen (N) to maintain crop yield, but its utilization efficiency is not high. Chemical nitrification inhibitors are used to improve N utilization efficiency, but they are expensive and need to be applied continuously. Biological nitrification inhibition (BNI), a phenomenon in which the plant itself secretes a nitrification inhibitor and exerts its effect, is expected to improve N utilization efficiency in agricultural ecosystems and reduce environmental loads. Many studies have been conducted on BNI plants, especially the tropical pasture grass “Brachiaria,” including the identification of brachialactone as a nitrification inhibitor. However, these studies have targeted rhizosphere soils that directly evaluate the effects of plant root secretions, and although there are many studies, there are very few reports on BNI effect in field experiments. Regarding the expression of BNI, it has been shown that sorghum is related to the suppression of ammonia-oxidizing archaea (AOA) (JIRCAS Research Highlights 2019, A05) but not fully elucidated in Brachiaria. On the other hand, at field scale, it is necessary to evaluate the entire field including not only the rhizosphere soil but also the inter-plant soil. This experiment clarifies the change in the nitrification rate of the bulk soil and its mechanism in the cultivation of tropical grass Brachiaria.

Seven varieties of Brachiaria grasses (with different BNI potentials in root exudates) and a bare plot were set as the control plot, and a field cultivation trial was conducted for 18 months at the Tropical Agriculture Research Front (TARF) of JIRCAS (Fig. 1). Among the seven varieties investigated, Tupy has the highest BNI activity in root exudate and Marandu has the lowest (Table 1). The potential nitrification rate in the inter-plant soil (center at 90 cm between stocks, depth 0 to 30 cm) after 18 months of Brachiaria cultivation differs depending on the variety, and among the 7 varieties investigated, 3 varieties (Marandu, Mulato, and Tupy) have particularly inhibited nitrification rates (Fig. 2), and the degree of decrease in the nitrification rate of each variety did not necessarily match the BNI activity of root exudates of each variety (Table 1). Since multiple regression analysis including BNI activity in root tissue enables significant regression, the effect of BNI activity in root tissue reflecting root turnover can be considered. The nitrification rates after 18 months of cultivation were positively correlated with the abundance of AOA in the soil but not with that of ammonia-oxidizing bacteria (AOB) (Fig. 3). The decrease in the number of AOA is the cause of the decrease in the nitrification rate. The study targeted soils collected between Brachiaria plants, so there is a possibility that stronger nitrification suppression occurs in the rhizosphere soil and in the vicinity of the plants.

From these results, the establishment of a crop rotation system utilizing Brachiaria can be expected because previous studies have reported an increase in subsequent crop yields after Brachiaria cultivation.

*(S. Nakamura, P.S. Sarr, Y. Ando, G.V. Subbarao)*



**Fig. 1. Picture of field experiment**

**Table 1. Root amount and BNI activities in root exudates and root tissues of seven Brachiaria cultivars**

Cultivar	Root amount kg DM ha <sup>-1</sup>	BNI activity	
		in root exudate ATU g <sup>-1</sup> DM day <sup>-1</sup>	in root tissue ATU g <sup>-1</sup> DM
	Marandu	849	2.0
Basilisk	1,147	18.3	174.5
Kennedy	488	24.4	207.0
Mulato	648	7.0	200.5
Mulato II	855	7.0	202.8
Tupy	699	46.3	208.6
Tully	1,109	17.5	183.2

ATU (allylthiourea unit): The inhibitory effect from 0.22 μM AT in an assay containing 18.9 mM of NH<sub>4</sub><sup>+</sup>

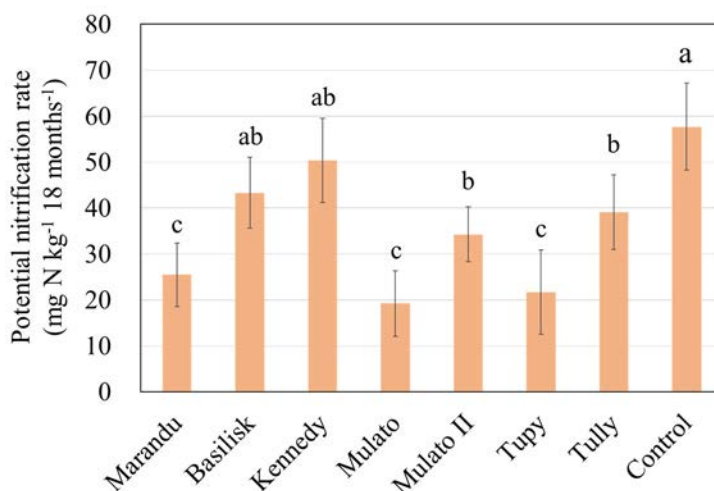


**Fig. 2. Cumulative nitrification rate in each treatment**

Error bar indicates standard error (n=3), different letters indicate significant differences by Tukey’s HSD method.

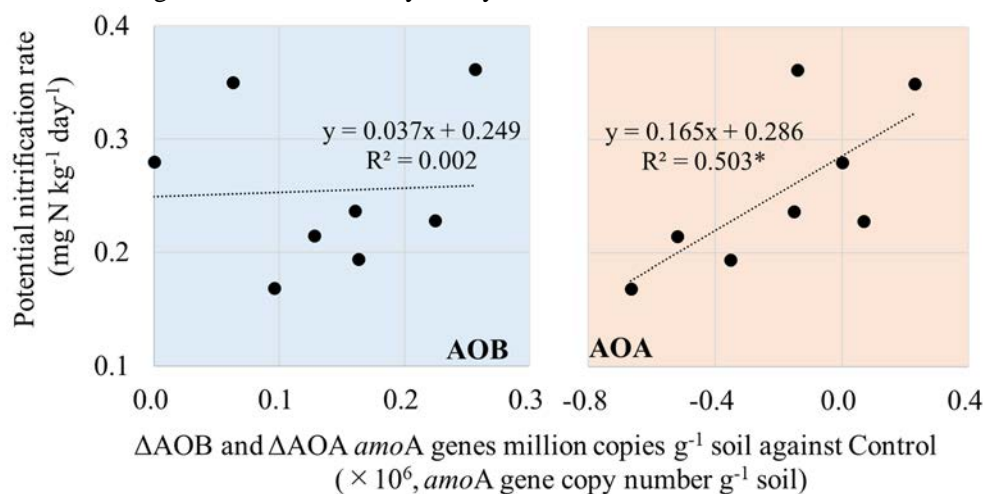


**Fig. 3. Relationships between potential nitrification rates and changes in AOB and AOA against Control**

## **The optimum application patterns of phosphate rock direct application under several agroecological zones for rainfed lowland rice cultivation in West Africa**

Phosphorus (P) is a finite resource that is difficult to reuse once it is released into the environment, in as much as P that is used in agriculture and flows into the ocean cannot be recovered. Studies for efficient P use in agriculture are being carried out internationally, especially in Africa where the use of local phosphate rock (PR) will be expanded as an affordable P resource. However, PRs in Africa are considered to be of low grade due to its low solubility and impurities such as quartz, iron, and aluminum, which are present in large amounts. Because local PRs are not sufficiently utilized, a solubility improvement technology through calcination has been studied (JIRCAS Research Highlights 2019). On the other hand, direct application of low-grade PR is expected to be effective in paddy rice cultivation, but the cultivation environment for rain-fed rice cultivation in Africa is diverse, and the application effect is uneven. Therefore, we investigated the effects of direct PR application in different agricultural ecological zones (AEZs) for rainfed rice cultivation for three years in West Africa and the optimum patterns for PR application with due consideration to the P use efficiency in each cultivation environment.

We have conducted PR application experiments in farmers' fields in three AEZs, namely, the Sudan Savanna Zone (SS), Guinea Savanna Zone (GS), and Equatorial Forest Zone (EF), representing the three cultivation environments of rainfed rice cultivation in West Africa. Table 1 shows the chemical properties of the surface soil of the rainfed paddy field in each AEZ. In each AEZ, a Non-P plot (NK), a PR direct application plot (PR), and a triple superphosphate application plot (TSP) was set up. Powdered PR obtained from the Kodjari deposit in Burkina Faso was used in this study. Each treatment plot was divided into a P continuous application plot and a residual effect plot in the second year. Non-P application was conducted in the third year (Fig. 1). In each year, rice grain yields and biomass were investigated.

Results showed that the yield ratio (RY) between the PR plot and the TSP plot increased in the order of  $SS < GS < EF$  with the difference in annual precipitation in the first application (Fig. 2). From the combination of fertilizer application frequencies surveyed, we selected one with high phosphorus use efficiency (PUE) and high relative agricultural efficiency (RAE) as the optimum application frequency for PR application in each AEZ. For SS and GS, "2 years continuous application following 1 year residual effect" and for EF, "1 year application following 2 years residual effect", the amount of PR application can be the minimum, and the same yield as the annual application can be obtained (Table 2).

*(S. Nakamura, F. Nagumo, S. Tobita, M. Fukuda [Central Region Agricultural Research Center, NARO (CARC)], T. Kanda [Institute for Agro-Environmental Sciences, NARO (NIAES)], R.N. Issaka [CSIR-Soil Research Institute (SRI)], I.K. Dzomeku [University for Development Studies (UDS)], S. Saidou [Environment and Agricultural Research Institute (INERA)], M.M. Buri [SRI], E.O. Adjei [SRI], V.K. Avornyo [UDS], J.A. Awuni [UDS], A. Barro [INERA], D. Jonas [INERA])*

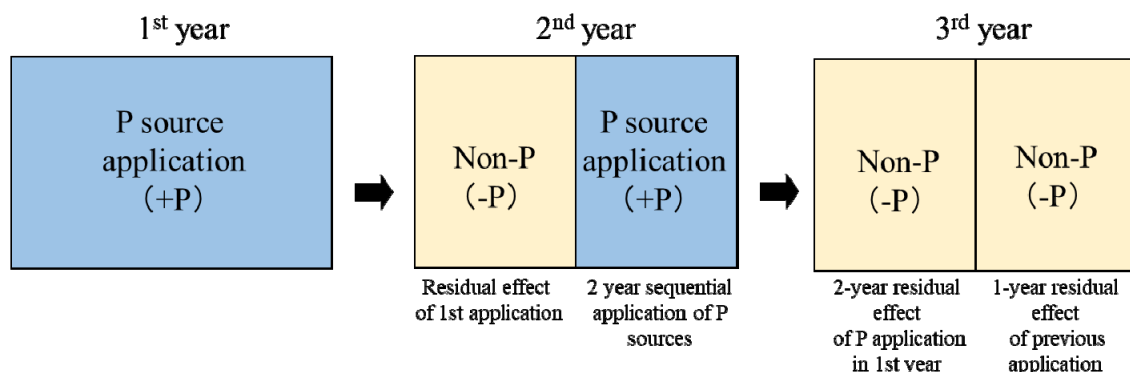


**Fig. 1. Outline of phosphate rock direct application experiment**

**Table 1. Surface soil chemical properties under each agroecological zone**

		Agroecological zone (AEZ)		
		SS	GS	EF
Annual precipitation	mm	800	1,100	1,350
pH (H <sub>2</sub> O)		5.40	5.72	5.12
Available P	mg P kg <sup>-1</sup>	1.90	8.51	4.99
Total C	g kg <sup>-1</sup>	7.73	4.31	10.34
Total N	g kg <sup>-1</sup>	0.58	0.41	0.82
Exchangeable Ca	cmolc kg <sup>-1</sup>	2.48	1.88	5.11
Exchangeable Mg	cmolc kg <sup>-1</sup>	0.93	1.11	2.01
Exchangeable K	cmolc kg <sup>-1</sup>	0.18	0.15	0.24

SS: Sudan savanna (Burkina Faso, Saria), GS: Guinea savanna (Ghana, Tamale), EF: Equatorial Forest (Ghana, Kumashi)

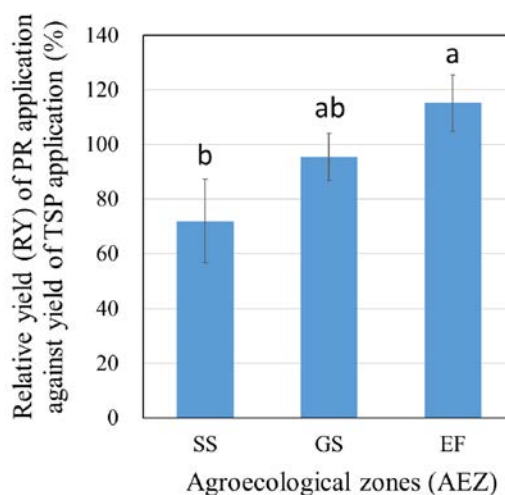


**Fig. 2. First year application effect of phosphate rock under each agroecological zone**

Error bars are standard error. Different alphabets indicate 5% significant difference by Tukey-Kramer method.

**Table 2. Phosphate rock direct application effect with several application patterns under each agroecological zone**

PR application patterns /Total phosphate application (kg P <sub>2</sub> O <sub>5</sub> ha <sup>-1</sup> 3 years <sup>-1</sup> )	Averaged rice grain yield (t ha <sup>-1</sup> year <sup>-1</sup> )			Relative agronomic efficiency <sup>†</sup> (RAE %)			Phosphate use efficiency <sup>††</sup> (kg kg P <sub>2</sub> O <sub>5</sub> <sup>-1</sup> year <sup>-1</sup> )			
	SS	GS	EF	SS	GS	EF	SS	GS	EF	
	-P -P -P	0	2.42 c	2.02 c	3.63 b					
+P -P -P	135	2.79 b	2.67 b	5.02 a	20.3	62.6	96.5	8.3	14.4	30.9
+P +P -P	270	3.65 a	3.13 a	4.99 a	69.6	84.6	84.9	13.7	12.4	15.2
+P +P +P	405	3.85 a	3.12 a	5.02 a	63.9	77.2	89.4	10.6	8.2	10.3

“+P/-P” indicates with and without P application in each year. Different alphabets denote 5% significant difference by Tukey-Kramer method.

†Relative agronomic efficiency (RAE): (Yield in PR – Yield in Control)/(Yield in TSP – Yield in Control) × 100

†† Phosphate use efficiency: (Yield in PR – Yield in Control)/Annual phosphate application rate



## Effect of rhizosphere soil addition on available phosphorus content in phosphate rock-enriched compost

The available phosphorus (P) content in sub-Saharan African soils is limited, representing a major constraint on agricultural productivity. Phosphoric fertilizers are used to correct soil phosphorus deficiency, but their high costs have prevented widespread adoption by African smallholder farmers. Phosphate rock, the primary material for manufacturing phosphoric fertilizer, is found in considerable quantities in several African countries, including Burkina Faso. Burkina Faso Phosphate Rock (BPR) is often co-composted with crop residues to enhance P availability through biological processes. Microbial materials are often used to promote P solubilization during the composting process, but it is difficult for many African farmers to obtain commercially available microbial inoculants. Here, we investigated alternative and smallholder farmer-friendly ways of improving P solubilization during composting by supplementing composts with rhizosphere soil as a microorganism source.

In this study, we prepared and monitored three compost types, sole compost, BPR-enriched compost, BPR-enriched compost + rhizosphere soil, for 180 days (Fig. 1). The C/N ratio was adjusted to 25/1 with urea, and the moisture content was maintained at 65% with regular watering. We examined the changes in available P fractions and the dynamics of P-solubilizing microbes, as well as the release of enzymes associated with P solubilization. At compost maturity (180 days), the combined number of P-solubilizing microbes (P-solubilizing bacteria = PSB and P-solubilizing fungi = PSF) in BPR-enriched composts was significantly higher in the treatment supplemented with rhizosphere soil (Fig. 2A). At this stage, the number of microbes producing P-solubilizing enzymes was also significantly higher in the BPR-enriched compost with soil (Fig. 2B). Among these microbes, those producing the alkaline phosphatase enzyme (*phoD*) were exponentially higher than those that release acid phosphatase and phosphonate (data not shown). The available phosphorus in composts significantly correlated with P-solubilizing fungi and alkaline phosphatase that dominate the microbes and the enzymes, respectively (Fig. 3). We observed no positive correlation between phosphate-solubilizing bacteria (PSB) and available P. The available phosphorus content (inorganic and organic phosphorus extracted with sodium hydrogen carbonate and water) in the BPR-rock-enriched compost was equivalent until the 60<sup>th</sup> day after the start of the composting. However, on the 180<sup>th</sup> day, although the difference was not significant, the available phosphorus content of the compost with the rhizosphere soil tended to be higher than when it was not added (Fig. 4). This result indicates that rhizosphere soil is a promising microbial consortium source to promote phosphorus solubilization during the composting process.

We confirmed through sorghum field trials that BPR-enriched compost with rhizosphere soil leads to yields equivalent to that of chemical fertilizer (NPK).

*(P.S. Sarr, S. Nakamura,  
M. Fukuda [NARO], E.B. Tibiri, A.N. Zongo, E. Compaore [INERA])*



**Fig. 1. Composting trial**

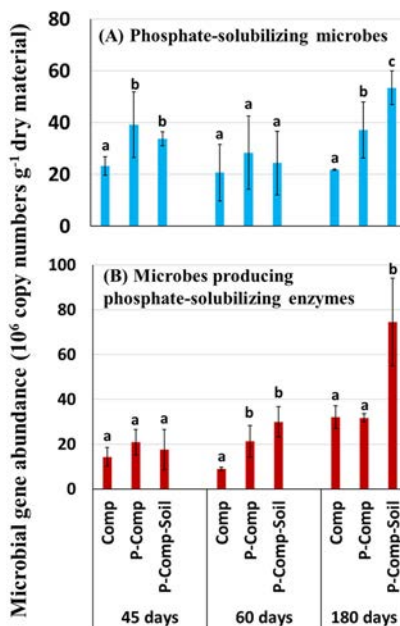


**Fig. 2. Changes in the abundance of phosphate-solubilizing microbes and phosphate-solubilizing enzymes during composting**

(A) Phosphate-solubilizing microbes = phosphate-solubilizing fungi + phosphate-solubilizing bacteria, (B) Phosphate-solubilizing enzyme-producing microbes = alkaline phosphatase-producing + acid phosphatase-producing + phosphonate-producing microbes. Alphabets that differ in each sampling period show a significant difference at  $p < 0.05$  by one-way ANOVA.

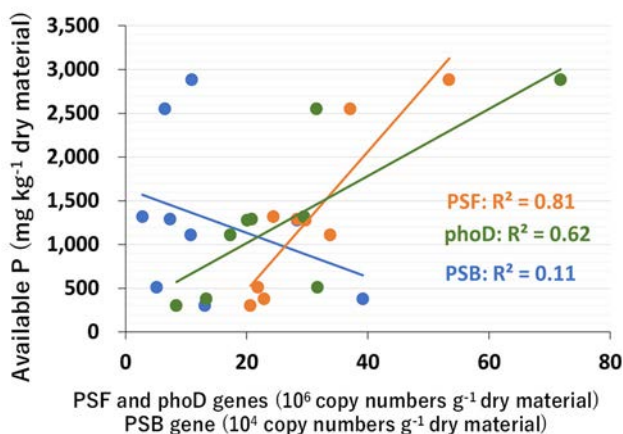


**Fig. 3. Relationships between the amount of available phosphorus and microbial gene abundance during composting**

- PSF: phosphate-solubilizing fungi,
- phoD: alkaline phosphatase-producing microbes,
- PSB: phosphate-solubilizing bacteria.

Sampling was performed on the 45<sup>th</sup>, 60<sup>th</sup>, and 180<sup>th</sup> day after the start of the composting. The data shown are the means for each type of compost over each period.

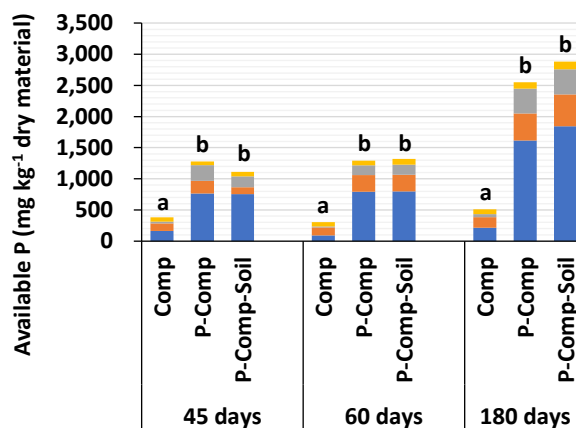


**Fig. 4. Transition of available phosphorus fractions during composting**

■ NaHCO<sub>3</sub>\_Po: sodium bicarbonate-extracted organic phosphorus, ■ NaHCO<sub>3</sub>\_Pi: Sodium hydrogen carbonate-extracted inorganic phosphorus, ■ H<sub>2</sub>O\_Po: water-extracted organic phosphorus, ■ H<sub>2</sub>O\_Pi: water-extracted inorganic phosphorus. At each period, different alphabets indicate a significant difference at  $p < 0.05$  following one-way ANOVA.

## **Introducing a quantitative trait locus, *MP3*, improves rice panicle numbers in nutrient-poor soils**

The majority of paddy fields in sub-Saharan Africa (SSA) are characterized by nutrient-poor soils. In such fields, tillering in rice plants is severely restricted, which results in a reduced number of panicles and thus a decrease in grain yield. Therefore, genetic improvement to increase rice tillering may ensure sufficient panicles in nutrient-poor soils and thus lead to increase in rice productivity. Because we previously detected a quantitative locus, *MP3* (*MORE PANICLES 3*), to be effective at increasing the number of panicles in nutrient-rich fields, we expected that *MP3* will also be effective in enhancing rice productivity in nutrient-poor soils.

In this study, we used a high-yielding *indica* cultivar, Takanari, and its near-isogenic line bearing the *MP3* allele derived from a *japonica* cultivar, Koshihikari (NIL-*MP3*). They were first grown in pots that contain nutrient-poor soils from Madagascar at various P application rates. The pot experiment demonstrated vigorous tillering in NIL-*MP3* compared to Takanari from the early vegetative stage even under low P levels (Fig. 1). We next conducted multiple field trials in Madagascar with a total of 12 experimental conditions using the two varieties. The experiments produced grain yields ranging from 1.3 to 4.1 t ha<sup>-1</sup> and panicle numbers ranging from 107 to 270 m<sup>-2</sup>. The results revealed that NIL-*MP3* produced a greater number of panicles and spikelets m<sup>-2</sup> (19% and 12%, respectively) than Takanari, with grain yields ranging from 2.0 to 4.1 t ha<sup>-1</sup>, but not in extremely low yield environments (< 1.3 t ha<sup>-1</sup>) (Fig. 2).

The results of this study indicate that *MP3* is effective at increasing the number of panicles in nutrient-poor soils in SSA. However, utilization of *MP3* in conjunction with fertilizer management may be necessary in extremely low yield environments (< 1.3 t ha<sup>-1</sup>). We are currently introducing *MP3* into a local Madagascar cultivar, X265, which is adapted to the environments in SSA, to verify the effect of *MP3* on grain yield in such environments.

*(T. Takai, Y. Tsujimoto, H. Asai, T. Nishigaki, T. Ishizaki, M. Sakata [Kochi University], N. Rakotoarisoa [National Center of Applied Research on Rural Development, Madagascar])*

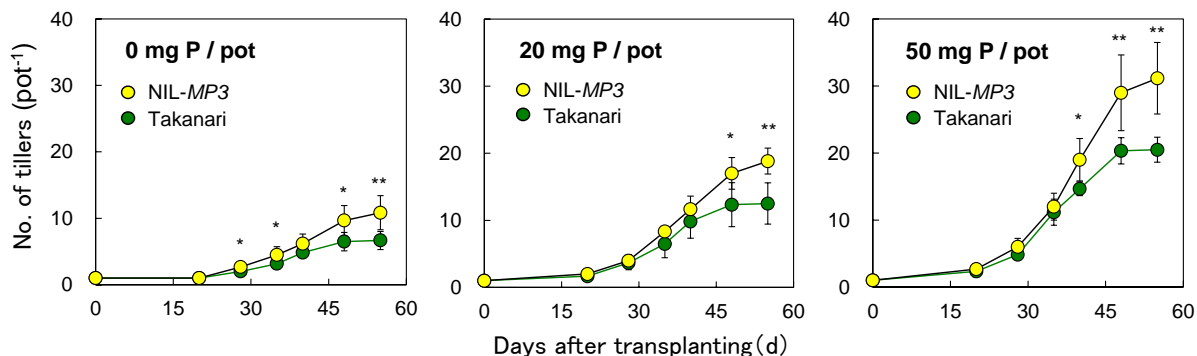


**Fig. 1. Changes in the number of tillers between Takanari and NIL-MP3 grown in pots that contain nutrient-poor soils in Madagascar at various P application rates.**

\*\* and \* show significance at 1% and 5% levels, respectively.

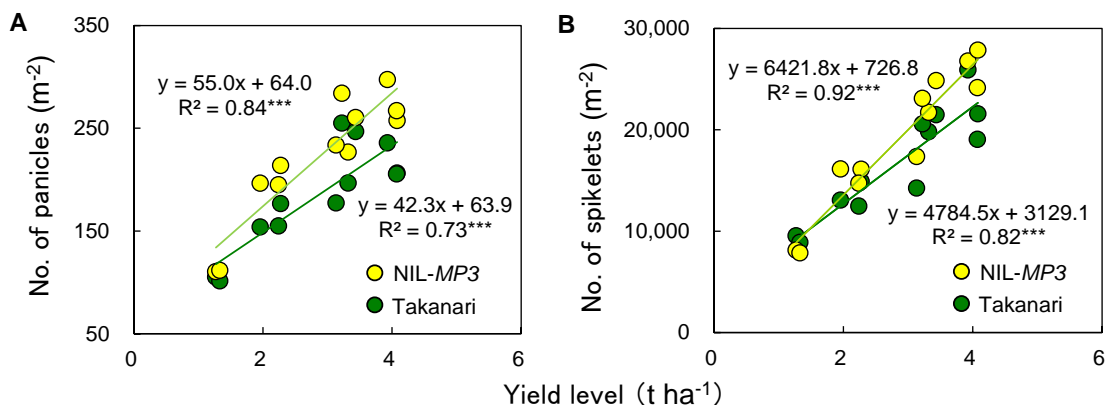


**Fig. 2. Comparison of the number of panicles (A) and spikelets (B) between Takanari and NIL-MP3 across 12 field experiments in Madagascar**

Yield level shows mean yield between Takanari and NIL-SPIKE in each experiment.

\*\*\* shows significance at 0.1% level.

## Dipping rice seedlings in phosphorus (P)-enriched slurry at transplanting increases yield and avoids cold stress under P-deficient soils in the tropics

Phosphorus (P) deficiency is a major yield constraint for lowland rice production in Sub-Saharan Africa. Plant P uptakes are restricted not only by low P content in soils but also by high P-fixing capacity with abundant Al- and Fe-oxides in soils in the region. To overcome this constraint, we examined the effect of dipping seedling roots into a P-enriched slurry before transplanting (P-dipping) as shown in Figure 1.

First, we identified that initial rice growth can be substantially improved by the P-dipping (Fig. 2). The optimal duration of dipping and the P concentration in the slurry are less than 2 hours and 1.8%–2.6%, respectively. We further clarified that P-dipping can facilitate plant P uptakes by creating a soluble P hotspot at the plant base or near the root zone even in high P-fixing soils where P incorporation has no effect on rice growth (Fig. 3). Then, subsequent on-farm trials confirmed that P-dipping can significantly increase both grain yield and applied P use efficiency in the typical P-deficient lowlands of Madagascar (Fig. 4). The effect of P-dipping was particularly significant at a high-elevation and cool climate site, where the improved grain fertility is attributable to the avoidance of cold stresses at the reproductive stage because the technique shortens days to heading by 14 days compared to control (no fertilization) and by 6 to 9 days compared to conventional P application via broadcast.

Because lowland rice production in Sub-Saharan Africa is widely subjected to environmental stresses such as low temperature, water shortage at the end of the rice growing seasons, and highly P-deficient soils, P-dipping can be an efficient P fertilization technique for resource-limited farmers in the region.

*(Y. Tsujimoto, A.Z. Oo, K. Kawamura, T. Nishigaki, N. Rakotoarisoa [FOFIFA])*

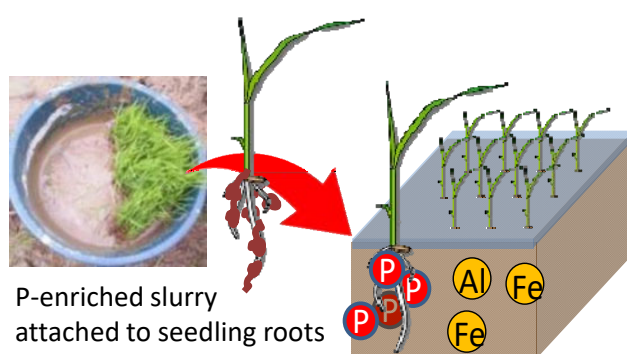


**Fig. 1. An illustration of the P-dipping technique**

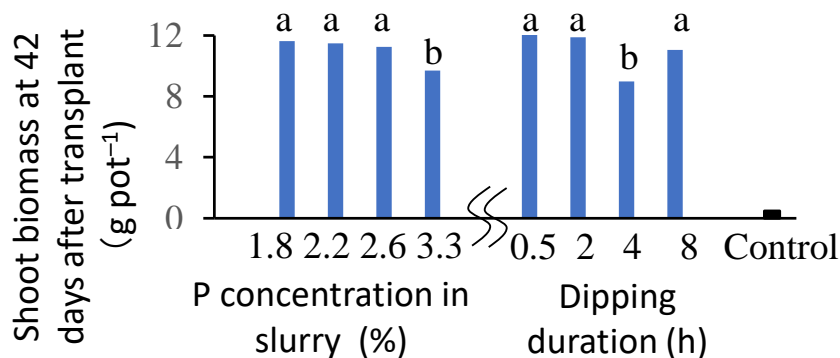


**Fig. 2. Effect of P concentration in slurry and duration of P-dipping on initial plant growth**

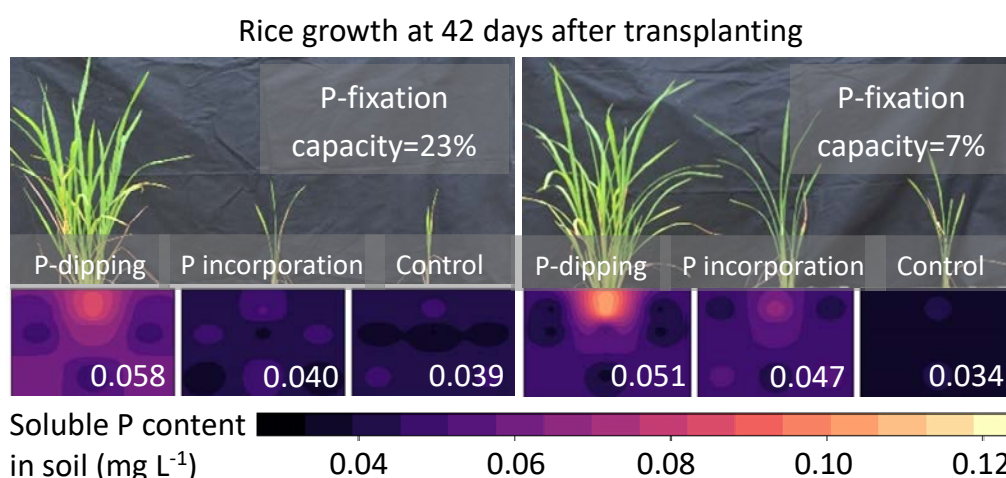


**Fig. 3. Effect of P-dipping on plant growth and spatial distribution of soluble P content in the soils differing in P-fixing capacity**

Both P-dipping and P incorporation treatments applied P at 40 mg pot<sup>-1</sup>. The numeric number in the spatial map indicates the average soluble P content (mg L<sup>-1</sup>) in the pot.

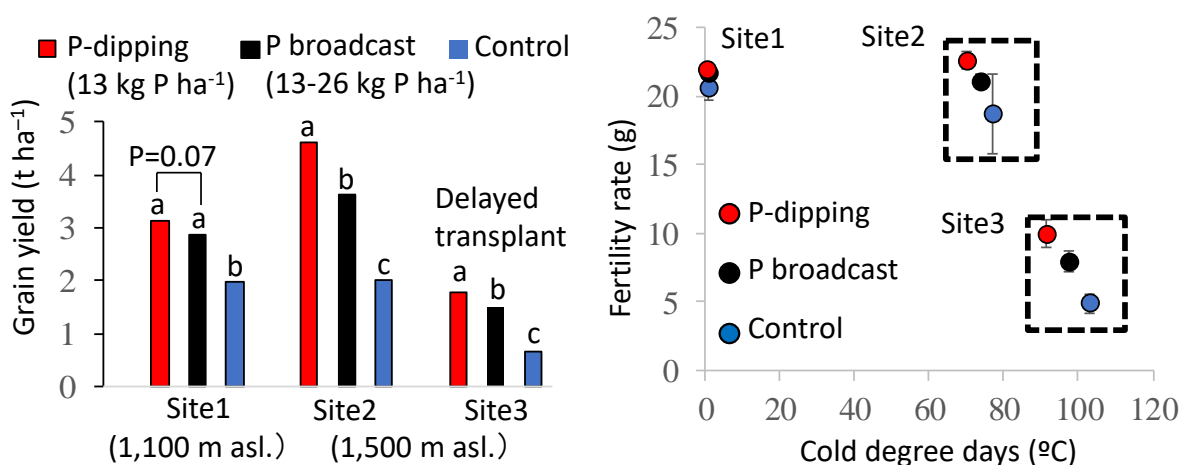


**Fig. 4. Effect of P-dipping on grain yield and on cold degree days and fertility rate**

Cold degree days is the sum of daily mean temperatures below 22 °C from 15 days before to 7 days after heading. Fertility rate is the product of filled grain weight and filled grain rate.



## **Selection of a Diversity Research Set to facilitate efficient genetic and breeding studies of Guinea yam (*Dioscorea rotundata*)**

Yam, the common name for crop species belonging to the genus *Dioscorea*, is widely cultivated as a staple crop in tropical and sub-tropical regions. West Africa, which accounts for 95% of the world's annual yam production (approximately 54 million tons) recognizes the important role of yam in regional food security and income generation. Guinea yam (*D. rotundata*, Fig. 1) is the most cultivated species in this region, representing majority of the total yam production. While *D. rotundata* is one of most important crops in West Africa due to its long growth cycle, large plant size, dioecy, inconsistent flowering habit, polyploidy, and a high level of heterozygosity, activities related to genetic research and breeding have been limited. To facilitate efficient utilization of plant genetic resources and promote genetic research and breeding of this crop, the *Dioscorea rotundata* Diversity Research Set (DrDRS) was developed. The DrDRS is a subset with a small number of accessions representing the genetic diversity of a core collection of *D. rotundata* accessions, the largest collection of this species worldwide.

In general, the so-called “non-redundant collection” such as Diversity Research Sets representing the genetic diversity of the original collection plays a vital role in facilitating efficient utilization of plant genetic resources. This is particularly relevant for vegetatively propagated large plant size tuber crops with a long growing period such as *D. rotundata*, to enable researchers to conduct detailed research more efficiently. In this study, a total 102 accessions were selected as DrDRS from the available 447 accessions, which serve as the base collection and are maintained at the International Institute of Tropical Agriculture (IITA), using the simple sequence repeat (SSR) markers we developed (JIRCAS Research Highlights 2015, B05). DrDRS retains the same level of genetic diversity as the base collection (Fig. 2 and Table 1). The average Shannon's diversity index with respect to 21 morphological traits of DrDRS and base collection (1.138 and 1.114, respectively) suggested that a similar level of morphological diversity was also captured within the DrDRS. The accessions of DrDRS showed a wide range of variation in basic agronomic traits such as growth period, number of tubers per plant, yield per plant, and average tuber weight. This variation was considerable when compared with the variation observed among the 10 lines/genotypes conventionally used in the breeding program at IITA (Fig. 3).

The DrDRS accessions could serve as a working collection to broaden the genetic variation for use in practical breeding programs as well as in future genomic analyses using the genome information of *D. rotundata* (JIRCAS Research Highlights 2017, B02) aimed at the genetic improvement of *D. rotundata* in West Africa. The DrDRS is expected to facilitate the development of excellent varieties that make effective use of the wide range of genetic diversity of this crop.

(S. Yamanaka, S. Muranaka, H. Takagi, B. Pachakkil [Tokyo University of Agriculture], G. Girma, R. Matsumoto, R. Bhattacharjee, M. Abberton, R. Asiedu [International Institute of Tropical Agriculture], M. Tamiru-Oli, R. Terauchi, [Iwate Biotechnology Research Center])



**Fig. 1. Cultivation of Guinea yam in West Africa (left) and harvested tubers (right)**

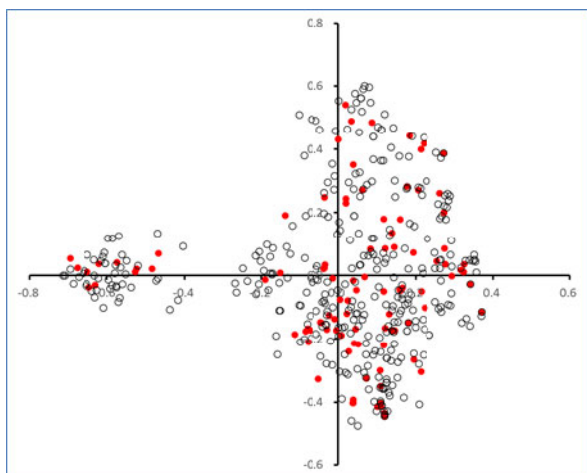


**Fig. 2. Distribution of base collection (open) and DrDRS (red) on the principal coordinate analysis plot based on SSR variation**

**Table 1. Genetic diversity indices in base collection and DrDRS through analysis of 16 SSR markers**

	<i>Na</i>	<i>Ho</i>	<i>He</i>	PIC
Base (n=447)	96	0.373	0.583	0.549
DrDRS (n=102)	94	0.383	0.563	0.529

*Na*: number of alleles, *Ho*: observed heterozygosity, *He*: expected heterozygosity, PIC: polymorphic information

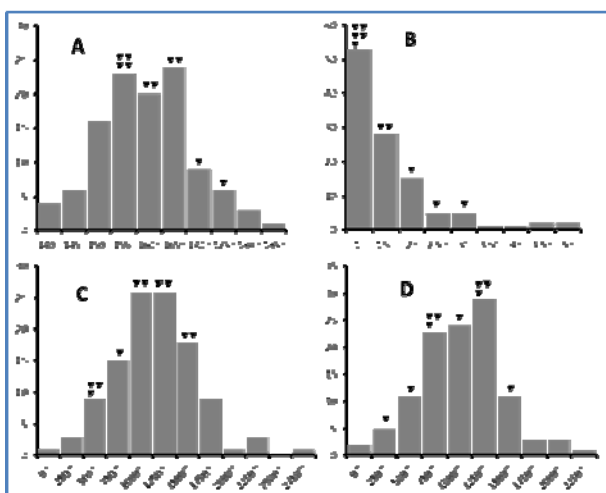


**Fig. 3. Variation of basic agronomic traits in DrDRS**

A: Growth period (days to harvest), B: Number of tubers per plant, C: Yield per plant (g), D: Average tuber weight (g) Arrowhead: distribution of ten IITA breeding materials.

## Variety selection for improving cowpea production under multi-environmental conditions in the Sudan Savanna

Cowpea (*Vigna unguiculata* (L.) Walp) is a legume crop widely grown in West Africa. Farmers traditionally cultivate cowpea as a low-cost and high-quality protein source and as a major cash crop. The primary production area is located between 600 and 900 mm yr<sup>-1</sup> isohyet, which roughly corresponds to the semi-arid region in the Sudan Savanna. However, the average yield is substantially below the biological potential, and yield vulnerability has been a cause of food insecurity in this region. One of the yield constraints is unstable meteorological conditions, especially low precipitation, causing drought stress. However, the occurrence of agricultural drought is not only determined by precipitation but also by soil type. Therefore, both climate and soil type should be considered in genotype selection and distribution.

To identify environmental and plant factors underlying this yield variation and select cowpeas with a stable yield, the grain yield variation of 16 cowpea genotypes in three dominant soils in the Sudan Savanna (Fig. 1) were analyzed in two consecutive years with different precipitation levels. In this study, the three soils were located near each other at the experimental site and thus the meteorological conditions were assumed to be identical for the soil types. The result showed that grain yield was largely different between years even for the same soil type, indicating no single genotype achieved both stable and high yields across these soil types (Fig. 2). In 2016, which had higher precipitation than the average year, variety J showed the highest grain yield across all soil types, while in 2017 with normal precipitation, different varieties showed the highest grain yield depending on the soil type. Based on this result, environment was defined as each combination of year and soil type, and this was subsequently analyzed through an additive main effect and multiplicative interaction (AMMI) model to detect the effects of the environment, genotype, and genotype-environmental interaction (GEI) on grain yield variation. The AMMI model uncovered two cowpea genotypes with stable and higher basal yields across all environments (variety G and variety P in Fig. 3); however, the grain yields of these genotypes were not the highest in each environment. Selection of a genotype with a medium but stable yield would be favorable to improve long-term average yield in the Sudan Savanna, where multiple soils with a large GEI are distributed in mosaic patterns.

The variety selection process employed in this study could be applied also for other regions with different annual precipitation in the Sudan Savanna where the three soil types investigated in this study are widely distributed, although historical cultivation data including sufficient annual rainfall variation is needed for analysis. This method reveals cowpea varieties or genotypes with stable yields for each of the environment and enables increase of cowpea production on a long-term-basis. To further improve cowpea production, appropriate cultivation practices such as fertilizer application and ridge planting may be determined depending on the soil type.

(K. Iseki, K. Ikazaki, J.B. Batiemo [National Institute of Environment and Agricultural Research])

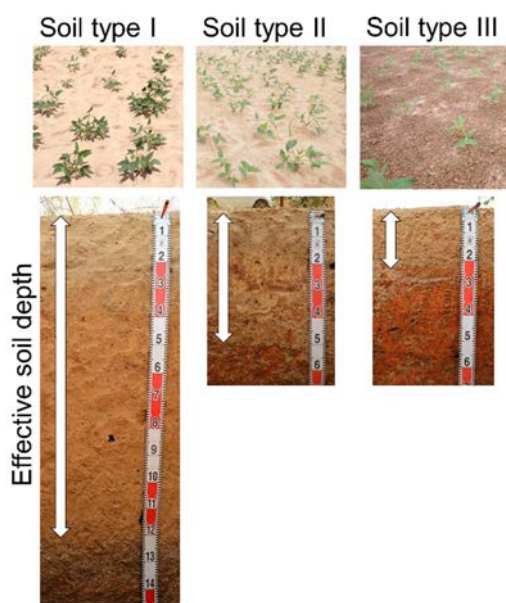


**Fig. 1. The three predominant soil types in the Sudan Savanna**

Each soil type has a different effective soil depth (rooting depth represented by the arrows). Soil type I > type II > type III in terms of soil depth, soil fertility, and water retaining capacity.

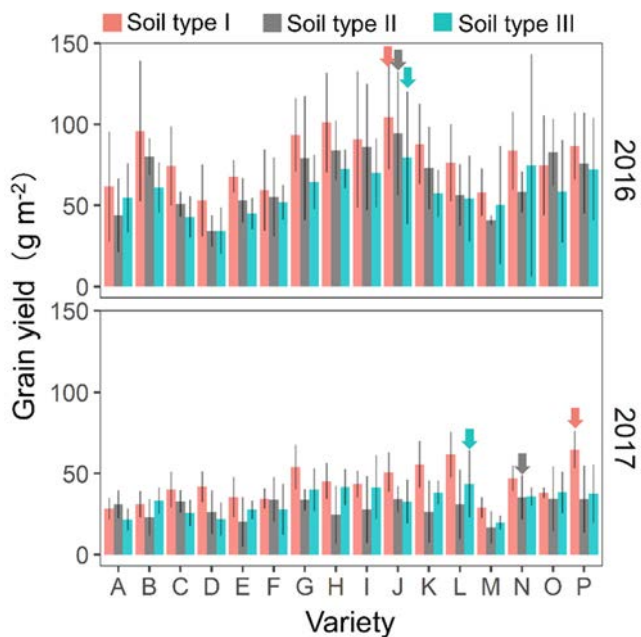


**Fig. 2. Grain yield of the 16 cowpea varieties (A-P) used in this study**

Bars are means  $\pm$  standard deviations for five replications. The arrows indicated the variety of highest grain yield at each of the soil type. Annual precipitation was 999 mm and 795 mm in 2016 and 2017, respectively.

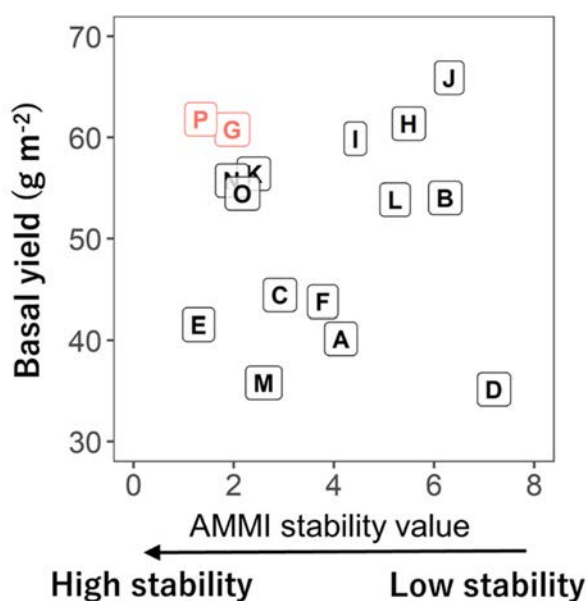


**Fig. 3. Yield stability of the 16 varieties under the environments defined by the soil types and annual precipitations**

The x-axis represents the AMMI stability value. The varieties with lower values have higher yield stability among the environments. The y-axis represents the genetically determined basal yield of each variety. The varieties G and P indicated by the red color have higher stability and higher basal yield at the same time.

## **Feeding of fermented TMR prepared with local feed resources improves milk production and profitability in Mozambique**

In Sub-Saharan Africa, feed shortages during the dry season are a major factor restricting livestock production. In Mozambique, which is located in Southern Africa, ruminants graze mainly on native grasslands and are customarily raised in combination with supplementary feeding of crop residues. However, this feeding method could not meet the nutritional requirements of dairy cows, and feeding them low-quality roughage adversely affects milk production. Therefore, locally available feed resources are expected to be used for preparing fermented total mixed ration (TMR) and improving livestock raising methods to promote the revitalization of local animal husbandry and improve the livelihoods of local people.

Fermented TMR was prepared in Mozambique with locally available feed resources including grass, crop by-products, and formulated feed using the simple plastic bag storage method (Fig. 1). Ten Jersey dairy cattle aged 3 to 4 years old with an average weight of  $336.6 \pm 19.8$  kg were used for a livestock feeding experiment. Fermented TMR prepared with Napier grass (*Pennisetum purpureum* Schmach), corn bran, wheat bran, and formula feed, was found to be rich in nutrients such as crude protein and crude fat, and can meet the nutritional needs of Jersey dairy cattle (Fig. 2). After 14 days of fermentation, the pH value of the fermented TMR was as low as 3.9, the ammonia nitrogen content was less than 0.01% of fresh material (FM), butyric acid and propionic acid were not detected, while lactic acid was produced in FM 1.0%. According to the criteria for evaluation of silage, the fermented TMR showed good fermentation quality (Table 1). Compared with the traditional diet, dairy cattle fed with TMR had better palatability, and the intake, dry matter digestibility, milk production, and profitability were significantly ( $p < 0.05$ ) improved (Fig. 3).

As an application of this result, the available sealing materials and feed resources can be used to prepare fermented TMR in other tropical and subtropical regions during the rainy and dry seasons. By using TMR to improve the feeding method of dairy cows, milk production can be stably increased. One thing to keep in mind is that when the TMR prepared by this simple preparation method is stored for more than one month, it is necessary to pay attention to the occurrence of aerobic deterioration caused by damage to the plastic bag. In this study, only fermented TMR with high-moisture Napier grass as the main component was prepared, so it is necessary to compare and analyze the feeding effects of fermented and non-fermented TMR on dairy cows. In addition, these results are limited to the improvement of raising methods, and other factors that hinder the promotion of dairy farming, such as hygiene management, disease control, and breeding management require other improvement efforts.

(Y. Cai, Z. Du, S. Yamasaki, T. Oya, D. Nguluve [Mozambique Institute of Agricultural Research (IIAM)], B. Tinga [IIAM], F. Macome [IIAM])



**Fig. 1. Preparation (left), storage (middle) and dairy cattle feeding (right) on fermented TMR**

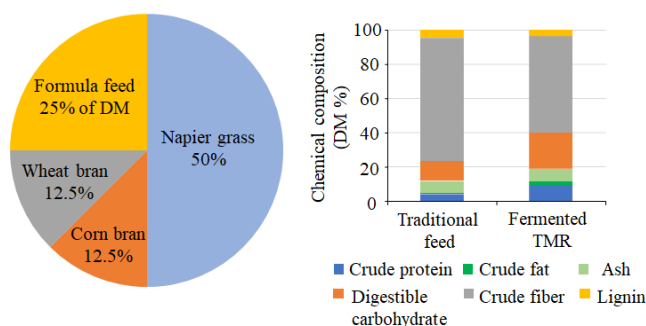


**Fig. 2. Ingredients (left) and chemical composition (right) of fermented TMR**  
 Digestible carbohydrate = carbohydrate – crude fiber – lignin.

**Table 1. Fermentation quality of TMR after 14 days of ensiling**

	Evaluation criteria	TMR material	Fermented TMR
pH	<4.2	6.2	3.9
Lactic acid, FM %	≧ 1.0	ND	1
Acetic acid, FM %	-	ND	0.3
Propionic acid, FM %	ND	ND	ND
Butyric acid, FM %	ND	ND	ND
Ammonia-N, FM %	<0.05	ND	<0.01

ND: not detected, FM: fresh matter.

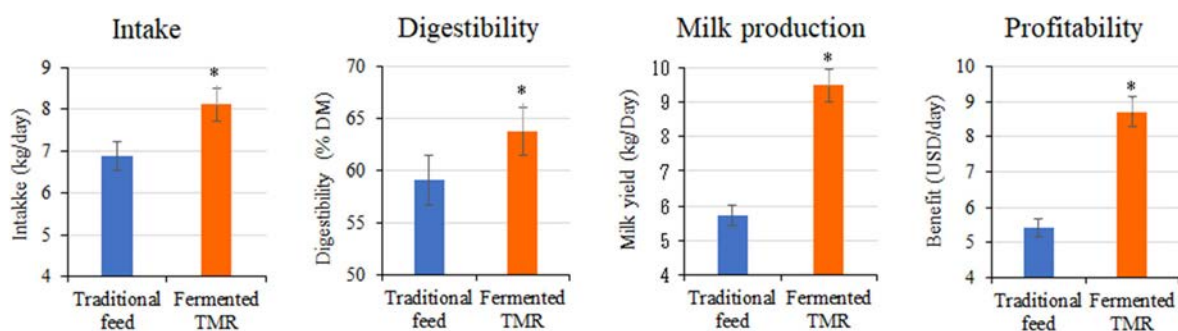


**Fig. 3. Performance of dairy cattle fed traditional feed and fermented TMR**

\*Means of five cattle differ significantly ( $p < 0.05$ ).



## **An integrated crop-livestock farm management model that can meet the reproductive conditions of dairy cattle in Mozambique**

In southern Mozambique, development programs have promoted the provision of exotic dairy cattle coupled with technical and marketing assistance to smallholder farmers to complement their cropping activities, improve income, and meet the increasing demand for milk products in the country. However, sustainable dairy production and integration with crop production is still limited. This study unravels the major constraints to sustainable dairy cattle farming in the Manhiça district of Maputo Province, where Jersey cattle was imported from South Africa and offered to farmers through development programs. To support farmers in making decisions, the study also develops an integrated crop-livestock farm management model to efficiently secure food and feed and improve income through crop-dairy interactions.

In addition to the three conditions regarding farmers' demands for food, risk management, and non-farm activities integrated into "A farm management model for assisting smallholder farmers in Africa" ([https://www.jircas.go.jp/en/publication/research\\_results/2018\\_b02](https://www.jircas.go.jp/en/publication/research_results/2018_b02)), the model developed in this study integrates the following conditions regarding dairy production: adequate feed supply that can satisfy the nutrient requirements of dairy cattle, proper herd structure that enables animal reproduction, and sufficient shed space (Fig. 1). Using a mixed integer programming method, the model is designed to simultaneously identify the optimal cropping system and dairy herd size to maximize total farm income while meeting food and feed requirements. From a structured questionnaire survey of all dairy cattle farmers in the Manhiça district (70 households), we found that the farmers face considerable difficulty in establishing a reproductive cycle due to high mortality and long calving interval of dairy cattle caused by infectious diseases and lack of artificial insemination (Fig. 2: red). The results of the model analysis applied to a representative dairy farm in the district show that once the calving interval is significantly shortened by reproductive improvement (Fig. 2: blue), the farm can keep three cows and one heifer calf and feed them enough to maintain actual productivity through effective use of crop residues, while producing enough food to meet household demands. Compared to actual farming, optimal crop-dairy farming (Table 1) will increase total income by 44%, or by 62% if the farm additionally processes the harvested raw milk into yogurt (Fig. 3).

The developed model can be used to i) support farmers' decisions to improve dairy cattle keeping and integration with crop enterprises, ii) support policy decisions to finance health and reproductive improvements of dairy cattle by informing the expected economic benefits to farmers, iii) identify the optimal dairy-crop interactions using newly developed cropping and/or feeding technologies along with their likely impacts on farmers' food security and income status.

*(J. Koide, T. Oya, T. Matsumoto, B. Tinga [Mozambique Agricultural Research Institute])*

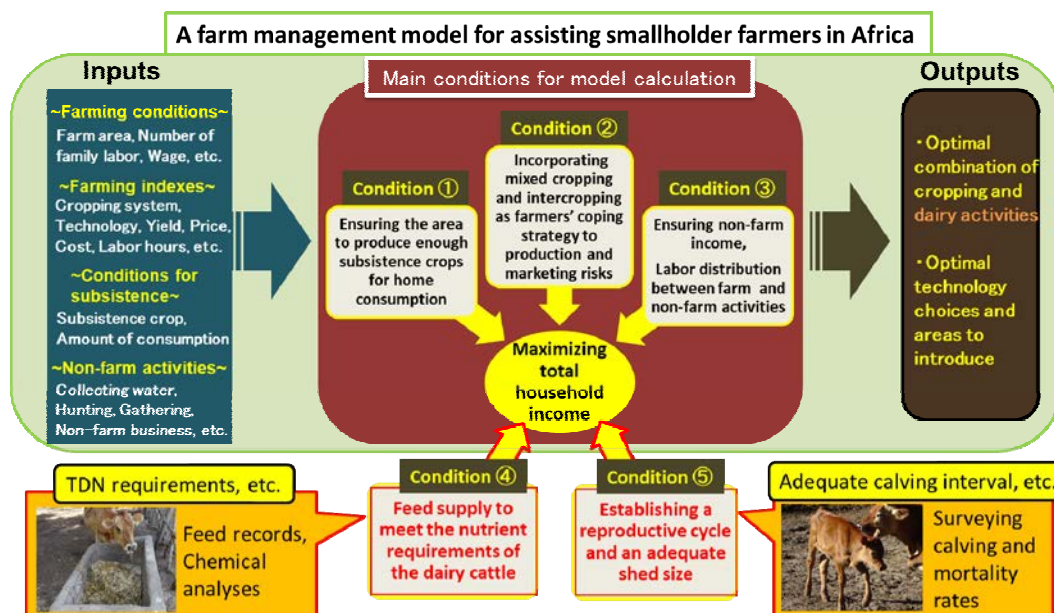


Fig. 1. An integrated crop-livestock farm management model developed in this study

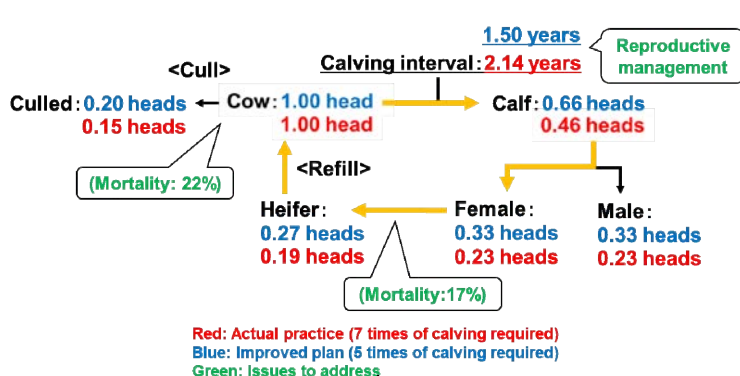


Fig. 2. Reproductive conditions of dairy cattle in the Manhiça district

Under the current conditions (red), for every heifer, 0.19 cows are refilled for succession per year, while 0.15 cows are culled given the mortality rate during the service (22%). This situation calls for seven offspring to maintain the herd, which takes about 15 years of service life with a calving interval of 2.14 years. If the calving interval is reduced to 1.5 years by reproductive improvement (blue), the required calving number becomes 5, and the service life is reduced to 7.5 years.

Table 1. Optimal cropping system and dairy herd size of a representative farm in the Manhiça district

		Actual	Optimal
Cropping (ha)	Cassava+Maize+Cowpea+Peanut+Pumpkin mixed cropping	0.22	0.24
	Maize+Cowpea+Peanut mixed cropping	0.33	0.32
	Maize+Sweet potato+Sugar cane+Pumpkin mixed cropping	0.48	0.70
	Maize+Sugar cane+Banana+Pumpkin mixed cropping	0.28	0.89
	Others	0.84	0
Dairying (head)	Jersey cow	1	3
	Jersey heifer calf	3	1

Actual: Actual crop and dairy farming by the farm

Optimal: Optimal crop and dairy farming identified by the model

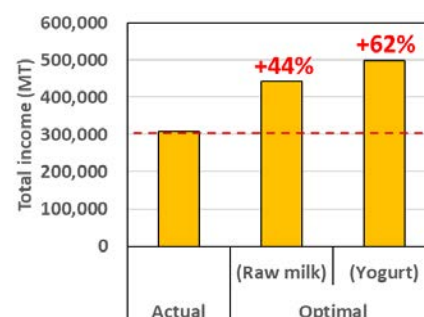


Fig. 3. Expected income increase by introducing optimal cropping system and dairy herd size

Actual, Optimal: Same as Table 1

MT: Metical (currency of Mozambique)

Rate of income increase is indicated above

## Key metabolites for estimating phosphorus use efficiency in rice

Phosphorus (P) is an indispensable macronutrient for plants, and it is widely applied as fertilizer to crop fields. However, the overuse of P fertilizers causes problems such as eutrophication of water bodies and depletion of P reserves on earth. In contrast, insufficient amounts of P fertilizers are often applied in developing countries due to their high cost. The development of more P-efficient crop varieties offers one avenue to increase yield in such environments. In our previous study, P use efficiency was investigated in a wide range of rice accessions collected from different regions of the world. This screening identified characteristic *Indica* rice accessions contrasting in P use efficiency, e.g., Taichung and IR64 (one of the major rice varieties in the world) have low P use efficiency, while Mudgo and Yodanya have high P use efficiency. In the current study, we hypothesized that P-efficient varieties have characteristic metabolic profiles that enable efficient use of P. To identify potential metabolites associated with high P use efficiency, plants were grown in a hydroponic culture containing different concentrations of P, and metabolic profiles were analyzed.

Based on the metabolomics data, a principal component analysis was conducted (Fig. 1). Under the P-deficient condition, metabolite profiles between the two groups (i.e., P-efficient and P-inefficient) were clearly separated, indicating that P-efficient and P-inefficient varieties have characteristic metabolite signatures. We next aimed at identifying key metabolites that distinguishes the P-efficient and P-inefficient variety groups. Our statistical analyses using LIMMA and ANOVA indicated key metabolites whose abundance is significantly different between the two groups. Notably, these metabolites were previously unassociated with P metabolism, implying that identification of these metabolites may shed light on basic molecular mechanisms of P use efficiency in rice. We further adopted a logistic Ridge regression model, which is a multi-variate analysis to predict a binary classification, and demonstrated that these key metabolites are indeed effective in predicting P use efficiency. Based solely on the contents of 14 key metabolites (such as benzoate and threonine; Fig. 2), P use efficiency (high or low) of 7 other rice varieties could be predicted successfully.

This study identified characteristic metabolite signatures for P-efficient varieties, whose usefulness was further validated through logistic regression analysis. Because analyses of P use efficiency from a large number of plants are cumbersome, identification of these key metabolites shall accelerate the selection of P-efficient accessions without the need for actual assessment of P use efficiency, and thus, boost rice breeding targeting efficient use of P. Based on the result of this study, we suggest that 1) metabolites serve as important molecular markers for complex trait that is difficult to assess, and 2) phenotypes can be predicted through combination of metabolite analysis and statistical modeling. In addition, the key metabolites may serve as the basis for further elucidation of the molecular mechanisms for P metabolism and P use efficiency.

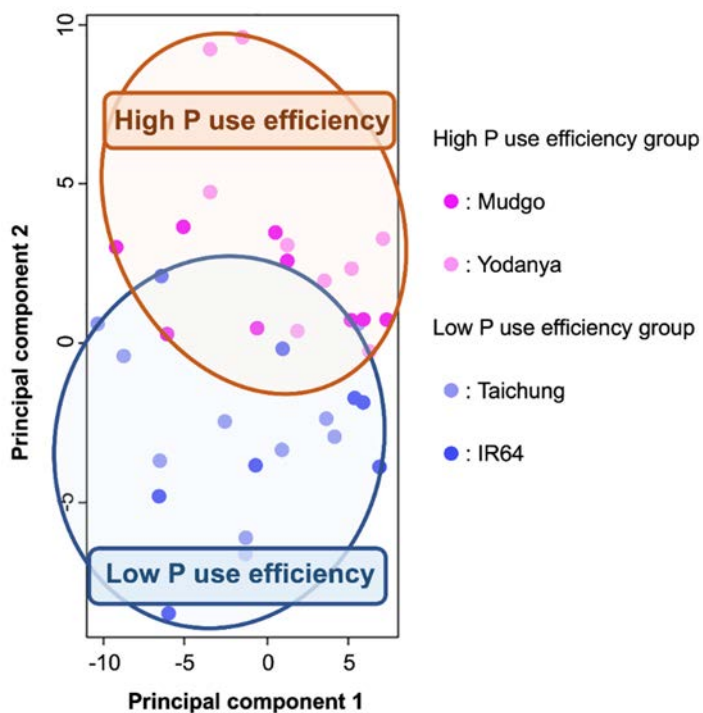


**Fig. 1. Metabolite profile of rice varieties contrasting in P use efficiency**

Result of principal component analysis based on the foliar metabolite content of the plants grown under P-deficient condition is shown.

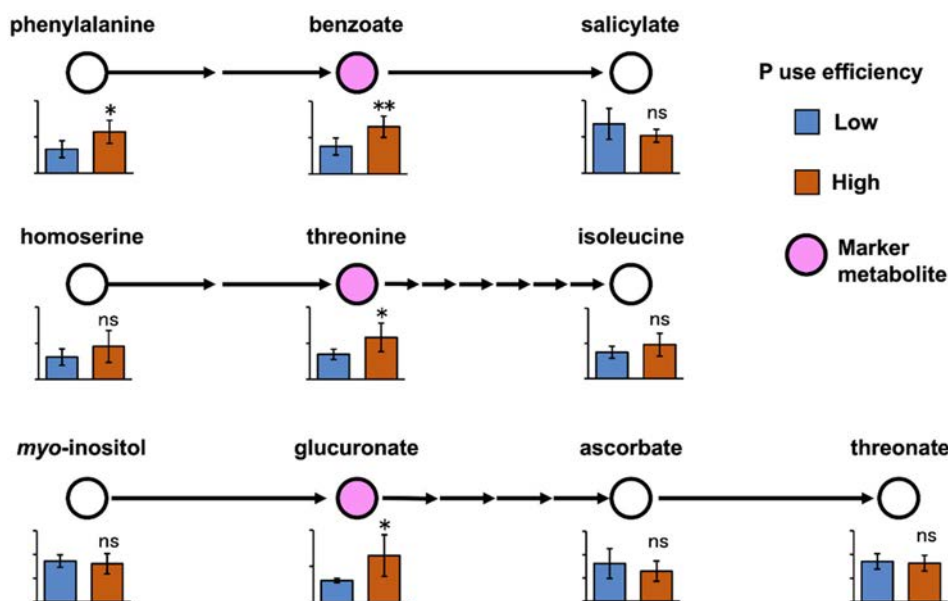


**Fig. 2. Marker metabolites for P use efficiency and related metabolic pathways**

Examples of metabolic pathways involving marker metabolites and their relative contents are shown. \*\* and \* indicate statistical significance at 1% and 5% levels (by *t* test).

(M. Wissuwa • Y. Ueda [Crop, Livestock and Environment Division], K. Kondo [Research Institute of Rice Production & Technology Co., Ltd.], M. Watanabe • T. Tohge [Nara Institute of Science and Technology], S. Ishikawa [Institute for Agro-Environmental Sciences, NARO], A. Burgos • Y. Brotman • A.R. Fernie • R. Hoefgen [Max Planck Institute of Molecular Plant Physiology])

## Genetic and phenotypic variation of agronomic traits and salt tolerance among quinoa inbred lines

*Chenopodium quinoa* (quinoa) has been recognized as a key crop with great potential for improving global food security due to its outstanding nutritional properties and ability to tolerate abiotic stresses such as drought and high salinity. However, a genome complexity derived from allotetraploidy and a genetic heterogeneity resulting from partial outcrossing have hampered genetic analysis of quinoa over the years. We established a standard inbred quinoa accession Kd and were first in the world to provide the draft genome sequence (2016 Research Highlights: Draft genome sequence of an inbred line of *Chenopodium quinoa*, an allotetraploid pseudocereal crop with high nutritional properties and tolerance to abiotic stresses). Moreover, an understanding of the genotype-phenotype correlation between comprehensive inbred lines will bring about advances in molecular breeding and research due to the molecular elucidation and genetic improvement of quinoa.

To evaluate genetic diversity in quinoa, we genotyped 5,753 single nucleotide polymorphisms (SNPs) in 136 inbred lines using Genotyping-by-Sequencing (GBS) based on next-generation sequencing. Our quinoa inbred lines were classified into three genetic sub-populations, corresponding to northern highland, southern highland, and lowland sub-populations using STRUCTURE, a neighbor-joining phylogenetic and principal component analysis. We also assessed salt tolerance and important growth traits (1,000-grain weight, plant height, stem diameter, leaf dry weight, seed yield per plant, and days to flowering) and generated a heatmap that provides a succinct overview of the genotype-phenotype relationship between inbred quinoa lines. Most lowland and southern highland lines were able to germinate even under high salinity conditions. In addition, most lowland lines displayed larger plant sizes and late flowering phenotypes, indicating that lowland lines are more suitable for growth in a temperate climate than the other lines.

The heatmap of the phenotypic traits, combined with the phylogenetic tree, provides quick access to the genotype-phenotype state of each quinoa line. We will therefore be able to accelerate the development of climate-resilient quinoa through efficient molecular breeding and research.

(Y. Kobayashi, Y. Fujita, N. Mizuno [Grad. Sch. Agri., Kyoto Univ., present affiliation: NARO], M. Fujita [RIKEN CSRS], S. Fukuda [Fac. Agri., Tottori Univ., present affiliation: Ishihara Sangyo Kaisha, Ltd.], K. Tanaka, T. Tanaka, H. Mizukoshi [Actree Co. Ltd.], E. Nishihara [Fac. Agri., Tottori Univ.], Y. Yasui [Grad. Sch. Agri., Kyoto Univ.]

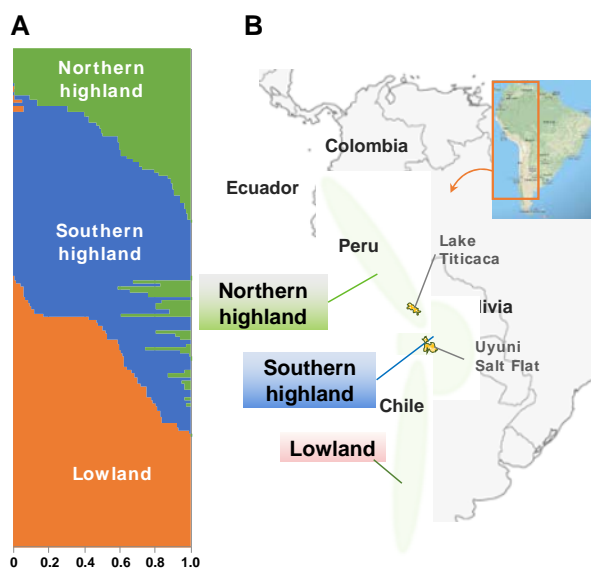


**Fig. 1. Population structure of quinoa inbred lines based on SNP genotype data** (A) Each quinoa line’s genome is represented by each bar on the y-axis, and the colors of the bar indicate the proportion of estimated membership in the three sub-populations. Lines having <80% of inferred ancestry from any one group are identified as an admixture. (B) Distribution of quinoa grouped into northern and southern highland and lowland sub-population in South America

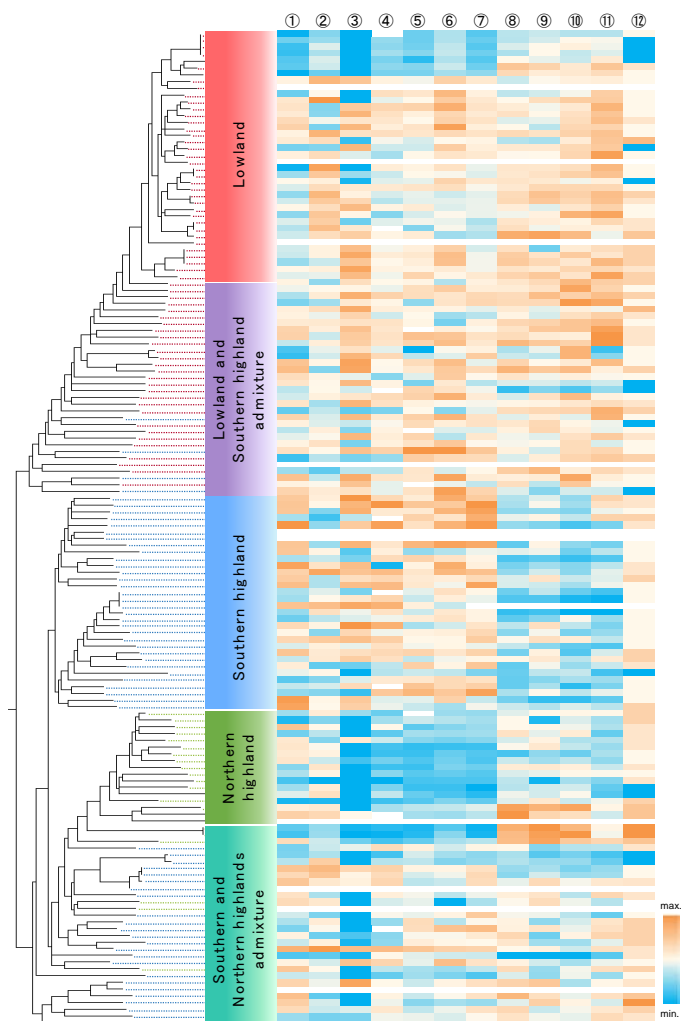


**Fig. 2. Heatmap of the phenotypic traits combined with the phylogenetic tree of quinoa inbred lines**

①-③: the average total hypocotyl and root length (mm) of seeds treated with 0, 300, and 600 mM of NaCl for 24 hours, 4 days, and 16 days, respectively; ④-⑦: thousand grain weight (g) during 2014-15 (Tsukuba), 2015-16 (Tsukuba), 2016 (Tsukuba), 2016-17 (Tottori); ⑧: plant height (cm); ⑨: stem diameter (mm); ⑩: leaf dry weight (g); ⑪: seed yield per plant (g); ⑫: days to flowering

**A behavior-predictive model based on thermoregulatory behavior of the desert locust in Africa**

There is an urgent need to develop better forecasting capacities so we can anticipate how species of economic importance will respond to environmental change. Pest insects are one of the most economically important groups of species requiring forecasting capacity. Any efforts to predict environmental constraints on the behavior, distribution, and abundance of terrestrial ectotherms such as insects must adequately capture how environment and behavior interact to determine body temperature, because virtually all biological processes are temperature-dependent. This is a significant challenge due to the complex, nonlinear responses of heat exchange between organisms and their microclimates, but it is possible to compute such responses from first principles using techniques in biophysical ecology.

The desert locust, *Schistocerca gregaria*, is one of the world's most destructive pest insects. Sometimes, desert locust populations grow explosively, forming swarms and causing locust plagues. A plague can affect up to 20% of the earth's surface across Africa, the Middle East, and Southwest Asia. Desert locusts can potentially damage the livelihoods of a tenth of the world's population. The preventive approach seeks to monitor and spray locust breeding areas. However, this is difficult in practice as many of the principal breeding zones are located in remote areas and are difficult to reach. We have been studying the locust and are developing efficient and sustainable control measures with due consideration to environmental well-being. For example, we have found that gregarious nymphs actively migrate during the day (Fig. 1), while they remain on relatively large plants during night under fluctuating thermal conditions. If we can understand these behavioral patterns and thermoregulatory behaviors, we can develop a predictive model. To obtain these ecological information and to develop a predictive model, we have taken temperature data on desert locusts doing different activities and their circumstances in the Mauritanian fields.

Using a thermal infrared camera in the field, we showed that gregarious nymphs altered their microhabitats as well as their postural thermoregulatory behaviors to maintain a relatively high body temperature (nearly 40°C) (Figs. 1 & 2). We used our data (Table 1) to successfully parameterize a general biophysical model of thermoregulatory behavior that could capture hourly body temperature and activity at our remote site using globally available environmental forcing data (Fig. 3).

This modelling approach provides a stronger basis for forecasting thermal constraints on locust outbreaks under current and future climates. Our technique may prove especially useful if it contributes toward developing forecasting capacity and preventive control, both short-term in response to weather events and long-term in response to climate change.

(K.O. Maeno,

P. Cyril [The French Agricultural Research Centre for International Development (CIRAD)],

M. R. Kearney [The University of Melbourne])

S. Ould Mohamed [The Mauritanian National Anti-Locust Centre (CNLA)]



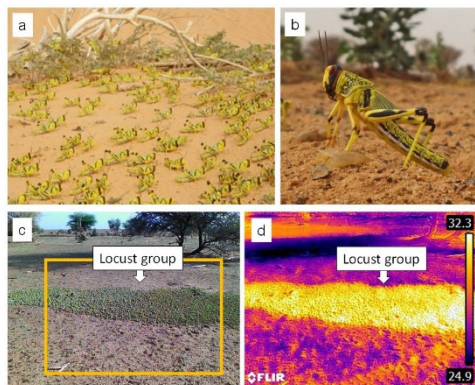


**Fig. 1. Behaviors of gregarious nymphs of the desert locust**

a: marching as a group, b: stiling behavior, and c: basking in the cool morning. Photo d shows thermal image of the basking locusts.

Description	Value
lethal maximum body temperature	50°C
lethal minimum body temperature	1°C
thermoregulation target body temperature	40°C
maximum foraging body temperature	43°C
minimum foraging body temperature	25°C
minimum basking temperature	15°C
minimum temperature for movement to basking site	15°C

**Table 1. Parameters used in the model for the desert locust hoppers**

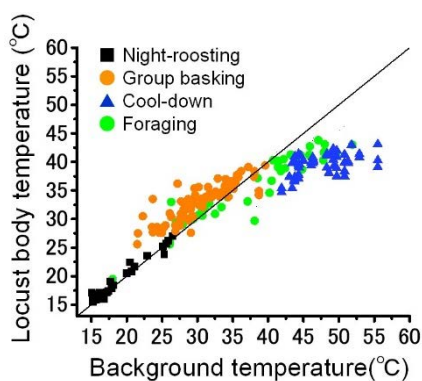


**Fig. 2. Relationships between background temperature and locust body temperature when locusts displayed various behaviors such as roosting on plants at night, group basking, cooling-down, and foraging**

		Predicted behaviors			
		Night-roosting	Group basking	Cool-down, foraging	Total
Observed behaviors	Night-roosting	37	0	2	39
	Group basking	0	5	90	95
	Cool-down, foraging	8	0	163	171
	Total	45	5	255	305
Accuracy (%)		82.2	100.0	63.9	

**Fig. 3. Confusion matrix of the observed vs. predicted behaviors of hoppers with the ectotherm-microclimate model**

## Healthy seedcane propagation and distribution manual against sugarcane white leaf disease

Sugarcane white leaf disease (SCWLD) is one of the most devastating diseases affecting sugarcane production in Asia. In Thailand, which is the world's second-largest exporter of sugar, SCWLD is considered to have the most serious effect on sugarcane production. The pathogen of SCWLD is phytoplasma, and effective treatments against SCWLD have not yet been developed. Two leaf hoppers, *Matsumuratettix hiroglyphicus* and *Yamatotettix flavovittatus*, are known as vector insects. From the results of our study in a severely infected commercial sugarcane field, the probability that the seedcane was already infected with SCWLD was high. Therefore, it was highly possible that healthy seedcane distribution was effective for reducing SCWLD occurrence. Sugarcane is a plant species grown through vegetative propagation. Its intergenerational propagation rate is low, multiplied only by a factor of approximately seven to ten per generation. Thus, to propagate a sufficient amount of healthy seedcane, a propagation system extending across multiple generations is required. On the other hand, healthy seedcane propagation in the spread area is difficult because vector transmission occurs frequently. In order to solve this problem, we developed the "Healthy seedcane propagation and distribution manual against SCWLD" for sugar mills and public institutions interested in healthy seedcane production.

The manual is composed of a preface and three chapters (Table 1). Chapter 1 describes a healthy seedcane propagation method and an effective seedcane distribution method. It also recommends that management techniques should be combined depending on the field sanitation level (Fig. 1). According to the results of the verification test, low-risk seedcane could be propagated by this technique (Figs. 2 & 3). Chapter 2 presents a simple protocol for SCWL disease detection using the loop-mediated isothermal amplification (LAMP) method. This method should be used "to obtain healthy seedcane as a source for propagation" and "to evaluate the latent disease probability." Chapter 3 describes a protocol for producing healthy seedcane using the tissue culture method. The products could be used as seedcane for the 1<sup>st</sup> propagation field.

This manual is available in both Thai and English. As a measure against SCWLD in each region in Thailand, domestic sugar factories in particular are expected to make use of the Thai language version in the production and distribution of healthy seedcane. The English version is similarly expected to be used not just in Thailand but also in other countries that are affected by SCWLD. In any case, users are advised to check and confirm current pesticide treatment regulations in their respective countries.

(Y. Kobori, S. Ando, Y. Hanboonsong [KhonKaen University], S. Sakuanrungrasirikul [Department of Agriculture, Thailand], W. Saengsai [Department of Agriculture, Thailand], S. Pituk [Department of Agriculture, Thailand], S. Kumhong [Department of Agricultural Extension, Thailand], T. Hamarn [Office of the Cane and Sugar Board])

**Table 1. Contents of the manual**

	Chapter title	Contents
Preface		Basics of SCWLD and purpose of this manual
Chapter 1	Propagation Field Management and Healthy Seedcane Product Distribution	Damage caused by the SCWLD, ecology of the pathogen and the vector Management of the healthy seedcane propagation field and efficient distribution methods of the products
Chapter 2	Experimental Protocol: Detection of SCWL Disease by LAMP Assay	Detection protocol of SCWLD pathogens from latent plants
Chapter 3	Protocol for Producing Disease-Free Sugarcane Seedlings Through a Tissue Culture Process	Disease-free sugarcane seedling production protocol by tissue culture techniques

Generation	Propagation stage	Field sanitation level	Field management*				
			Isolated field	Large area cultivation	Removal of diseased stalks	Pesticide treatment	Evaluation of the latent disease probability
G0	Tissue culture/Introduction from a low-risk region						
G1	1 <sup>st</sup> propagation field	AAA	○	○	2 times/month	○	○
G2	2 <sup>nd</sup> propagation field	AA	○	○	1 time/month	○	○
G3	3 <sup>rd</sup> propagation field	A	×	×	1 time/month	○	○

\* ○ : required    × : not required

**Fig. 1. Complete overview of the healthy seedcane propagation system**



**Fig. 2. Sugarcane in the verification test field for 1<sup>st</sup> propagation**

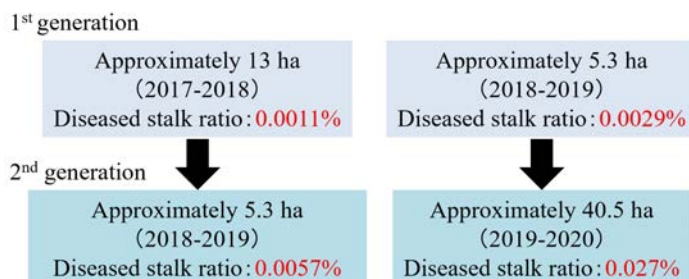


**Fig. 3. Results of the healthy seedcane propagation verification test**

These fields were managed following the propagation system described in Fig. 1. Compared to newly planted fields in the same region, disease prevalence was extremely low. The infection ratios of commercial sugarcane fields around the verification test area were 0% to 20% (from 32 fields, mean 5.8%: median 5%). Several farmers and sugar mills commended these products as acceptable and healthy seedcane.

## **International differential system to protect against rice blast disease**

Blast disease has been found to have caused serious damage to rice production in all areas of the world where rice is cultivated, from tropical to temperate regions. The use of resistance varieties is the most economically and efficient way to protect against rice blast disease in developing countries. The differential system, which can clarify the pathogenicity of blast isolates and resistance in rice cultivars, is a basic and important tool for breeding and pathological works. However, few countries or research institutes have used the differential system and applied the developed technology for crop protection.

To establish this protection system against blast disease in developing countries and regions, JIRCAS has conducted international collaborative research for developing and distributing the differential system in Asian and African regions.

Under the international research network, blast isolates and rice germplasm were collected. The pathogenicity of blast isolates using international differential varieties (DVs) and genetic variation of resistance in resistant rice cultivars were clarified. Based on these information, international standard differential blast isolates (ISDBIs) collected from different origins under the research network were selected (Table 1).

The ISDBIs and DVs comprise the international differential system, and the system is being used as the international standard for characterizing the pathogenicity of blast isolates and resistance of rice cultivars. It can also be applied to breeding works in rice cultivars and pathological studies for the development of a protection system.

Participants of the research network including Indonesia, Philippines, Vietnam, Laos, and Bangladesh also selected their respective local standard differential blast isolates, and these domestic differential systems were applied to breeding and pathological studies in each country.

One of the network's research achievements was the clarification of the wide variations in blast races (Fig. 1). The frequency of blast isolates virulent to DVs was clarified in each country and region and at the global level. The frequency of virulent blast isolates varied among DVs and regions. Particularly, high frequencies of wide-spectrum blast isolate virulence to DVs were found in Bangladesh and West Africa.

Furthermore, the highest diversities of blast races were found from Yunnan province, China, to Bangladesh. The diversities of blast races were corresponded with the those of resistance in rice cultivars. The relationships between blast races and rice varieties are explained by the gene-for-gene theory. The differential system will make it possible to characterize previous resistance genes and to find new genes, such as partial resistance genes, and provide access to the development of application methods for them in rice breeding. The information, i.e., the differential system and these new approaches, will contribute to the development of a durable protection system and for harmonizing agriculture with environment.

*(Y. Fukuta, H. Saito, M. Obara, S. Yanagihara, N. Hayashi [NARO])*

**Table 1. International differential system for rice blast disease**

Blast race	Differential variety and resistance gene in the genetic background																				Origin						
	LTH	IRBLsh-B	IRBLb-B	IRBLK69	IRBLa-A	IRBLF5	IRBLs-CP4	IRBLs-M	IRBLs-F5	IRBLkm-Ts	IRBL1-CL	IRBLsh-K3	IRBLk-kqLLT	IRBLip-K60	IRBL7-M	IRBL9-W	IRBLz-Fu	IRBLz5-CA	IRBLz-T	IRBLa2-PI		IRBLa2-Re	IRBL12-M	IRBLa-K1	IRBLa-CP1	IRBL19-A	IRBL20-IR24
	.	fish	P/b	P/t	P/a	P/l	P/3	P/5 (I)	P/k-s	P/k-m	P/t	P/k-h	P/k	P/k-p	P/7 (I)	P/9	P/z	P/z-5	P/z-t	P/ta-2		P/ta-2	P/12 (I)	P/ta-2	P/ta	P/ta	P/19 (I)
U62-i6-k000-z03-ta001	R	M	S	S	S	S	S	S	S	S	R	R	R	R	R	R	R	R	R	R	R	R	R	R	R	R	R
U63-i7-k157-z04-ta431	S	S	S	S	S	S	S	S	S	S	S	S	S	S	S	S	S	S	S	S	S	S	S	S	S	S	S
U63-i0-k100-z05-ta731	S	S	S	S	S	S	S	S	S	S	S	S	S	S	S	S	S	S	S	S	S	S	S	S	S	S	S
U03-i7-k177-z01-ta733	S	S	S	S	S	S	S	S	S	S	S	S	S	S	S	S	S	S	S	S	S	S	S	S	S	S	S
U23-i7-k177-z02-ta733	S	S	S	S	S	S	S	S	S	S	S	S	S	S	S	S	S	S	S	S	S	S	S	S	S	S	S
U61-i7-k100-z04-ta003	S	S	S	S	S	S	S	S	S	S	S	S	S	S	S	S	S	S	S	S	S	S	S	S	S	S	S
U73-i6-k111-z02-ta500	S	S	S	S	S	S	S	S	S	S	S	S	S	S	S	S	S	S	S	S	S	S	S	S	S	S	S
U53-i5-k157-z04-ta001	S	S	S	S	S	S	S	S	S	S	S	S	S	S	S	S	S	S	S	S	S	S	S	S	S	S	S
U41-i2-k100-z05-ta401	S	S	S	S	S	S	S	S	S	S	S	S	S	S	S	S	S	S	S	S	S	S	S	S	S	S	S
U01-i0-k073-z01-ta010	S	S	S	S	S	S	S	S	S	S	S	S	S	S	S	S	S	S	S	S	S	S	S	S	S	S	S
U01-i4-k143-z00-ta021	S	S	S	S	S	S	S	S	S	S	S	S	S	S	S	S	S	S	S	S	S	S	S	S	S	S	S
U23-i6-k157-z05-ta403	S	S	S	S	S	S	S	S	S	S	S	S	S	S	S	S	S	S	S	S	S	S	S	S	S	S	S
U03-i7-k137-z04-ta503	S	S	S	S	S	S	S	S	S	S	S	S	S	S	S	S	S	S	S	S	S	S	S	S	S	S	S
U73-i4-k102-z01-ta333	S	S	S	S	S	S	S	S	S	S	S	S	S	S	S	S	S	S	S	S	S	S	S	S	S	S	S
U23-i7-k155-z04-ta403	S	S	S	S	S	S	S	S	S	S	S	S	S	S	S	S	S	S	S	S	S	S	S	S	S	S	S
U43-i7-k173-z04-ta003	S	S	S	S	S	S	S	S	S	S	S	S	S	S	S	S	S	S	S	S	S	S	S	S	S	S	S
U01-i7-k177-z06-ta021	S	S	S	S	S	S	S	S	S	S	S	S	S	S	S	S	S	S	S	S	S	S	S	S	S	S	S
U73-i0-k000-z16-ta403	S	S	S	S	S	S	S	S	S	S	S	S	S	S	S	S	S	S	S	S	S	S	S	S	S	S	S
U73-i0-k100-z05-ta403	S	S	S	S	S	S	S	S	S	S	S	S	S	S	S	S	S	S	S	S	S	S	S	S	S	S	S
U53-i7-k100-z01-ta031	S	S	S	S	S	S	S	S	S	S	S	S	S	S	S	S	S	S	S	S	S	S	S	S	S	S	S
U63-i7-k100-z04-ta403	S	S	S	S	S	S	S	S	S	S	S	S	S	S	S	S	S	S	S	S	S	S	S	S	S	S	S
U71-i0-k101-z01-ta333	S	S	S	S	S	S	S	S	S	S	S	S	S	S	S	S	S	S	S	S	S	S	S	S	S	S	S
U63-i0-k153-z05-ta403	S	S	S	S	S	S	S	S	S	S	S	S	S	S	S	S	S	S	S	S	S	S	S	S	S	S	S
U23-i0-k104-z06-ta412	S	S	S	S	S	S	S	S	S	S	S	S	S	S	S	S	S	S	S	S	S	S	S	S	S	S	S
U23-i0-k177-z06-ta031	S	S	S	S	S	S	S	S	S	S	S	S	S	S	S	S	S	S	S	S	S	S	S	S	S	S	S
U63-i3-k102-z02-ta021	S	S	S	S	S	S	S	S	S	S	S	S	S	S	S	S	S	S	S	S	S	S	S	S	S	S	S

The international differential system consists of 25 differential varieties and the susceptible variety LTH, and 53 international standard blast isolates (Several blast isolates were omitted in the table). Blast race names were designated to each blast isolate selected according to the method of Hayashi and Fukuta (2009). Reactions: S: virulent (susceptible), M: moderate, R: Avirulent (resistant)

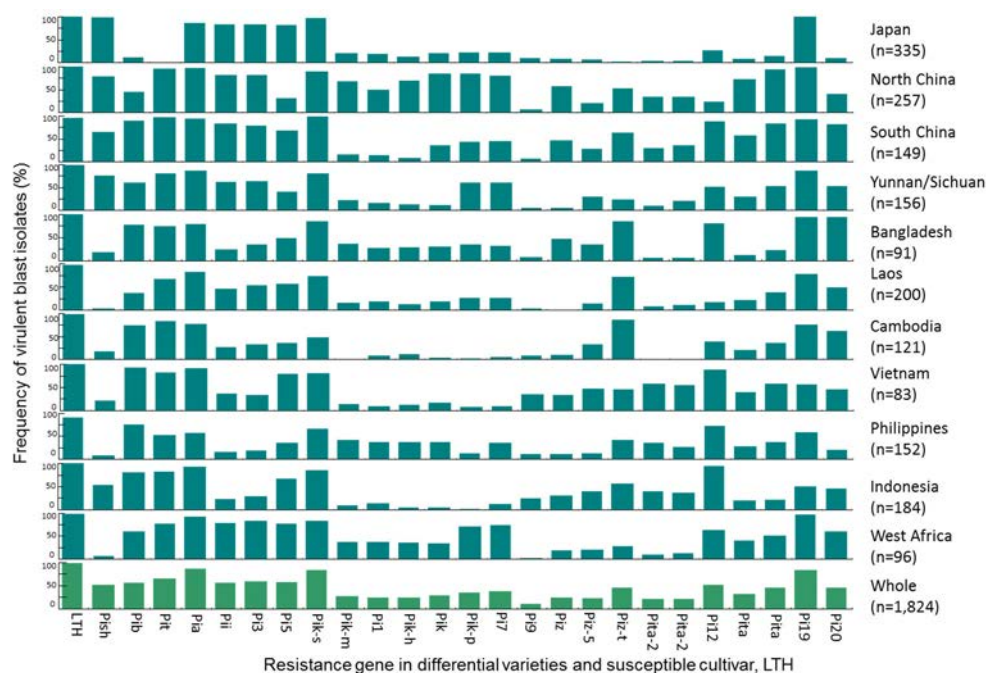


**Fig. 1. Frequency of virulent blast isolates to differential variety in each country and region**

Wide variations in virulent blast isolates to each differential variety were found, and they varied among regions. Wide-spectrum blast isolates virulent to differential varieties were found in Bangladesh and West Africa at high frequencies.

## **Effect of non-flooded water management on inside-canopy temperature dynamics, spikelet sterility, and grain yield of lowland rice in the tropics**

Increasing temperatures and water scarcity are concomitant threats to sustainable rice production in future climates. Although both aspects have been widely studied, little is understood about how water-saving management might affect heat-induced stress and grain yield of rice under open-field conditions. We implemented field experiments in four consecutive wet and dry seasons in the sub-humid tropics of northern Ghana to clarify how water management practices affect daily inside-canopy temperature ( $T_c$ ) dynamics, flowering time, heat-induced spikelet sterility, and grain yield of rice. Two rice varieties, IR64 and Jasmine85, were grown under two water regimes: 1) continuous flooding (Flooded), and 2) continuous flooding except for an approximately 20-day drainage treatment at the flowering period (Non-flooded). The Non-flooded treatment maintained high moisture contents above 60% of saturated volumetric water to avoid any significant drought stress. Inside-canopy temperature ( $T_c$ ) during the flowering periods were monitored at 2-minute intervals by placing MINCER (Micrometeorological Instrument for the Near-Canopy Environment of Rice) inside the canopy.

The effect of water regimes on grain yield and  $T_c$  differed significantly between the dry season (DS) and wet season (WS). Non-flooded management significantly reduced yields by 13–26% in the DS but not in the WS (Table 1). However, the effect of Non-flooded management on  $T_c$  at flowering time (0.2–0.3°C increase across varieties and years) (Figure 1) and spikelet sterility (3–5% increase) (Table 1) was relatively small even in the DS. In contrast, Non-flooded management greatly increased  $T_c$  from solar noon to midnight in the DS (Fig. 1).  $T_c$  did not differ between Non-flooded and Flooded treatments either at flowering time or nighttime in the WS (Fig. 1).

$T_c$  changes over the course of the day imply that Non-flooded management may have a higher risk of yield reduction in the DS of the sub-humid tropics by increasing late-afternoon-to-nighttime temperatures, which can cause physiological stress and respiration loss. The results can help improve water-saving management practices under contrasting climatic conditions in the sub-humid tropics and predict the combined effect of increasing temperatures and water scarcity on rice production.

*(Y. Tsujimoto, M. Yoshimoto, M. Fukuoka [National Institute for Agri-Environmental Sciences], A. Fuseini, Y. Inusah, W. Dogbe [Savanna Agricultural Research Institute, GSIR])*

**Table 1. Effect of water management on spikelet sterility and grain yield**

Variety	Water management	Spikelet sterility (%)				Grain yield (t ha <sup>-1</sup> )			
		Wet season		Dry season		Wet season		Dry season	
		2016	2017	2017	2018	2016	2017	2017	2018
IR64	Flooded	2.4 <sup>b</sup>	8.9 <sup>a</sup>	4.1 <sup>b</sup>	4.0 <sup>a</sup>	6.1 <sup>ab</sup>	5.2 <sup>a</sup>	6.1 <sup>b</sup>	6.3 <sup>b</sup>
	Non-flooded	2.3 <sup>b</sup>	5.9 <sup>a</sup>	7.5 <sup>ab</sup>	8.9 <sup>a</sup>	5.4 <sup>b</sup>	5.0 <sup>a</sup>	5.2 <sup>c</sup>	4.7 <sup>c</sup>
Jasmine85	Flooded	5.7 <sup>a</sup>	10.8 <sup>a</sup>	6.7 <sup>b</sup>	4.2 <sup>a</sup>	6.6 <sup>ab</sup>	5.6 <sup>a</sup>	7.4 <sup>a</sup>	7.7 <sup>a</sup>
	Non-flooded	2.6 <sup>b</sup>	8.2 <sup>a</sup>	11.8 <sup>a</sup>	7.2 <sup>a</sup>	7.0 <sup>a</sup>	5.5 <sup>a</sup>	6.4 <sup>b</sup>	6.4 <sup>b</sup>

Two varieties were allocated in 5.7 m × 4.5 m plots with 4 replicates, in different water management practices.

Different alphabets indicate significant differences at 5% by Tukey's HSD test.

\*Flooded: Continuously flooded from transplanting to maturity.

\*Non-flooded: Continuously flooded except for an approximately 20-day continuous non-flooded period, at around the heading dates of the two varieties. Volumetric moisture contents of soils were retained above 30% during the non-flooded period in all seasons except the dry season cultivation in 2018 in which volumetric moisture content went down to 26% due to the lack of irrigation water.

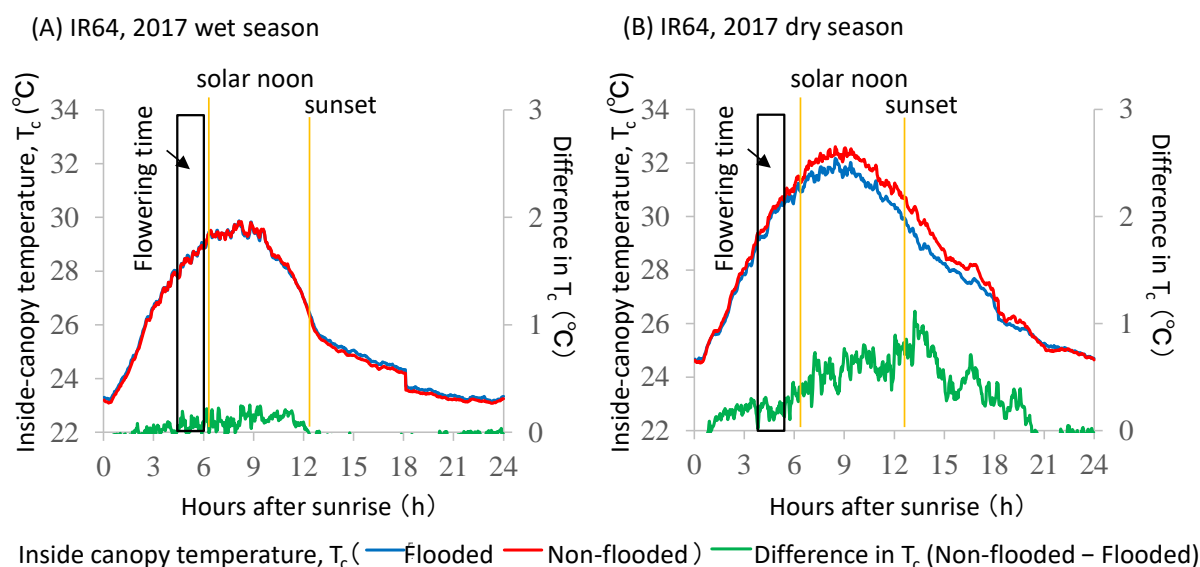


**Figure 1. Diurnal changes in inside-canopy temperature ( $T_c$ ) in the Flooded and Non-flooded water management and the  $T_c$  differences between these two management schemes for IR64 in the 2017 wet seasons and 2017 dry seasons**

The trend was equivalent for both varieties and in the other years.

The average of two replicates over peak flowering days (7 observation days around the day of 50% heading excluding any rainy days) is depicted. Grey bars within each figure indicate the period from initial to peak spikelet opening time which were determined by digital images taken at 10-minute intervals. Orange lines indicate the solar noon and apparent sunset time.



## **Designing a polyurethane-based husker roll for long-grain rice using a finite element model**

Rice husking is an operation where the husks are peeled from rough rice, and a rubber roll husker conventionally consists of two rubber rolls with different peripheral velocities that rotate to provide the shear stress needed to husk rough rice (Fig. 1). Both short- and long-grain rice, which have different shapes, affect rice husker performance, especially the husking ratio and wear of the husker roll. The performance with long-grain rice, which accounts for 80% of world rice production, is poorer than with short-grain rice.

We analyzed the fundamental mechanisms of the roll husker, and then compared the performance for long- and short-grain rice using a finite element model constructed based on high-speed camera observation.

A husking simulation based on the constructed model revealed that long-grain rice exhibited more accumulated friction loss (121.6 mJ) than short-grain rice (40.1 mJ) (Figs. 2 & 3). The difference in accumulated friction loss at the roll surface may lead to increased friction heat, which in turn induces wear. Since sufficient shear force is needed with rough rice to achieve a higher husking ratio, the optimum coefficient of friction and Young's modulus of the husker roll, which is related to viscoelasticity, for long-grain rice were calculated based on the model as being 0.8 and 8.1 MPa, respectively.

Newly designed polyurethane-elastomer-based husker rolls based on these results showed a better husking ratio and nearly 10 times greater durability than conventional rubber rolls in experiments undertaken in Thailand using long-grain rice (Table 1).

Roll huskers are the mainstream in commercial rice mills around the world, in terms of continuous operation and brown rice quality after husking. Their replacement rolls are commercially available as consumables, and the developed polyurethane-based husker roll is applicable to all roll huskers. Therefore, the results provide new opportunities to prepare new materials for the rice roll husker.

*(T. Yoshihashi; Y. Abe, N. Iwasaki, H. Sakanaka [Industrial Products Division, Bando Chemical Industry]; M. Fujinaka, R. Kido [Research Laboratories for Core Technology, Bando Chemical Industry])*

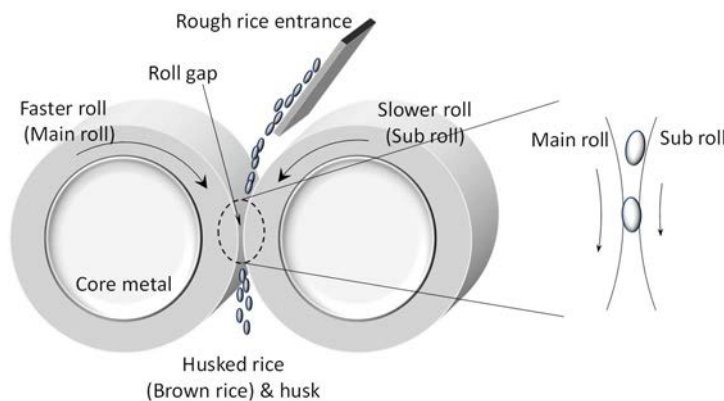


**Fig. 1. Schematic diagram of rice roll husker**

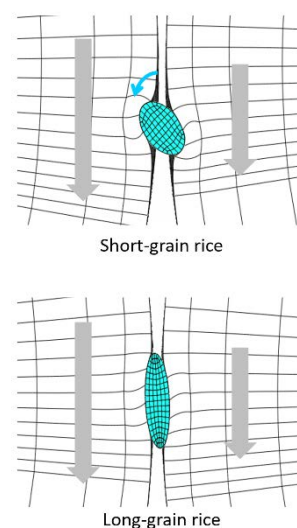


**Fig. 2. Differences between short- and long-grain rice in the roll gap**

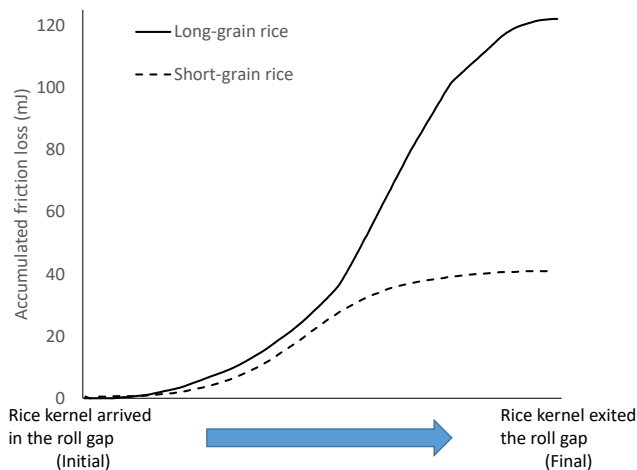


**Fig. 3. Accumulated friction losses for husking of single kernel**

**Table 1. Results from field husking tests at a rice mill in Thailand**

Husker roll	Viscoelasticity (tanδ, 90°C)	Coefficient of friction	Husking ratio	Broken rice ratio	Actual wearing	Estimated durability
Rubber roll (conventional)	0.089	0.514	77-85%	7-8%	10-10.5 mm at 10 hr	24-30 hr
Polyurethane-based roll designed for short-grain rice (commercial product)	0.021	0.544	55-61%	5-7%	5-7 mm at 1 hr	3.6-5 hr
Polyurethane-based roll designed for long-grain rice based on simulation results (improved)	0.035	0.699	82-88%	5-7%	7.3-7.4 mm at 72 hr	242-243 hr

## **Cost accounting for evaluating liquefaction of Thai fermented rice noodles and its prevention focusing on pH management**

Traditional Thai fermented rice noodles, *khanom jeen*, are produced and consumed widely in the nation as well as the Greater Mekong Subregion. A well-known problem with noodle production is sudden noodle liquefaction soon after production, severely affecting business and undermining buyer confidence. JIRCAS found that the increased pH level of *khanom jeen* noodles induced liquefaction; noodles with weak acidic (pH 6) or alkaline (pH 8) buffers result in liquefaction, while acidic (pH 4) buffers do not (Research Highlight 2017, C01 “Liquefaction of Thai fermented rice noodles can be prevented by maintaining the product in acidic condition of pH around 4”). Thus, managing the pH level can be a promising method for preventing noodle liquefaction.

We conducted simulation analyses, including cost-volume-profit analysis, to evaluate the effect of liquefaction on small-scale rice and noodle producers’ profitability and the cost of preventing the problem by focusing on pH management (Fig. 1). The results show that the instability of product quality, particularly noodle liquefaction, severely affects the profitability of flour and noodle producers (Fig. 2). Frequent pH level measurements at critical points of the production process can capture and prevent the risk of liquefaction. The cost for this is small (Table 1A), and simple to use digital meters are beneficial for measuring the pH of products at many different points. Incorporating practices to reduce high pH levels at appropriate points can reduce the risk of liquefaction. One approach is to wash the noodles with acid water (low pH) after the boiling process. The cost for this procedure is minimal and lower than using common food preservatives (Table 1B).

As mentioned above, the rudimentary management of the production process focusing on the pH level can secure product shelf life in the market and profitability. Note that the flour producer should adequately monitor and manage the fermentation, rather than merely reduce the products’ pH at the final stage. A high pH level of the products just after solid- or liquid-state fermentation indicates something abnormal in the process that needs corrective action through reviewing operations. The noodle producer needs to consider that the amount of acetic acid for washing noodles depends on each site’s water quality and the products’ flavor. The results of this study should not be generalized without carefully considering the businesses’ differences in technologies and capabilities, since the analysis is based on a small-scale noodles producer’s data.

*(E. Kusano, J. Marui, T. Yoshihashi)*

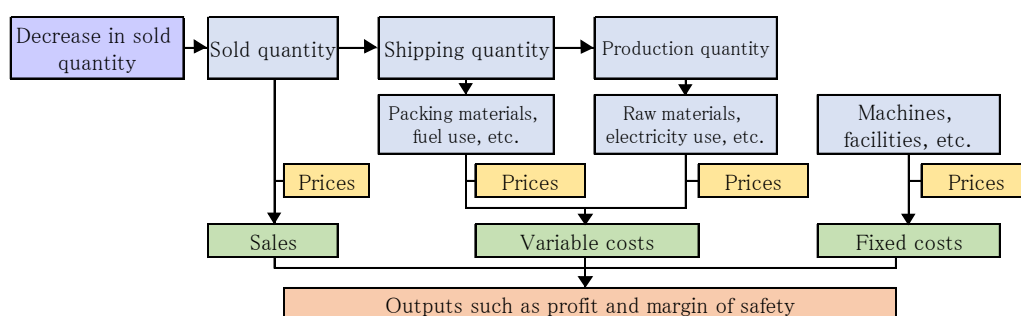


**Fig. 1. Conceptual chart of the simulation model**

Models for production of both the fermented rice flour and noodles are built based on the survey. The figure shows the common diagram for both processes.

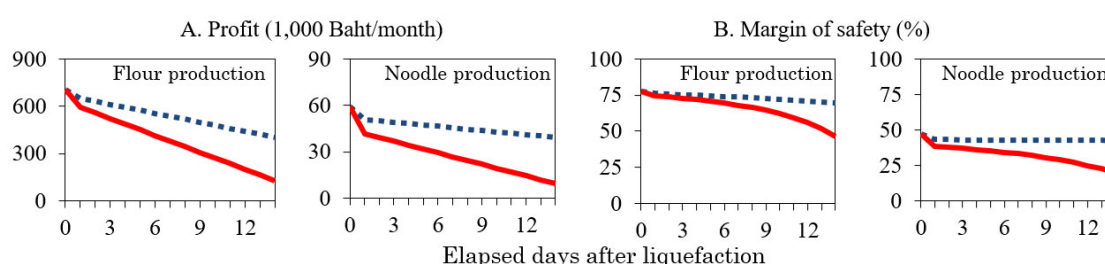


**Fig. 2. Estimated profit and margin of safety according to the decrease in sold quantity**

Solid line = 100% reduction in daily sales volume. Dotted line = 50% reduction in daily sales volume. “Noodle production” assumes that the process only uses purchased flour. It also assumes small businesses, an average size of fermented rice flour, and noodles producers registered with the Department of Industrial Works, Ministry of Industry (flour production: laborers = 13, raw material rice = 5.5 tons/day; and noodle production: laborers = 6, raw material flour = 0.6 tons/day). Only the sales volume is reduced on the first day, and the shipment and production volumes are also reduced to control variable costs on the second and subsequent days. The margin of safety measures the percentage decrease in monthly sales resulting in zero profit after the liquefaction.

**Table 1. Monthly average costs for preventing liquefaction focusing on pH management**

		For the surveyed company	For further pH management
A. Costs for measuring pH in the flour and noodle production processes by indicator papers	Measuring points (point/day)	10	20
	Costs (Baht/month)	373	746
	Percentage of total cost (%)	0.01	0.03
B. Costs for washing noodles by the water containing acetic acid	Volume of acetic acid (L/day)	0.2	1
	Costs (Baht/month)	216	1,083
	Percentage of total cost (%)	0.01	0.04

The surveyed company is the representative small-scale noodles producer, which uses a noodle-making machine that operates for 8 hours and produces 830 kg/day. The total cost for the surveyed company is 2.82 million Baht/month, with flour and noodle production accounting for 2.68 million Baht/month and 0.14 million Baht/month, respectively. The cost of measuring by pH meter is 431 Baht/month, assuming 6 years of durability. The cost of adding the maximum level of a common food preservative to noodles is 2,647 Baht/month.

**Discovery of *Capillibacterium thermochitinicola*, a thermophilic anaerobic bacterium that decomposes chitin**

Chitin, a type of polysaccharide contained in many organisms such as shrimp, crab, insects, shellfish, and mushrooms, is the second-most abundant natural biological resource on earth next to cellulose. It is expected to be used as a biomaterial such as fiber material and soil conditioner, but its poor solubility makes it limited to industrial use. Biomass containing chitin such as shrimp shells and crab shells from fish processing factories is discarded in large quantities. There are many microorganisms that have chitin-degrading enzymes, but no bacteria that can decompose and assimilate chitin in a thermophilic anaerobic environment have been found. Therefore, in order to make effective use of chitin-based biomass by microbial saccharification, we researched for thermophilic anaerobic bacteria that can efficiently decompose chitin in a high-temperature environment and clarified their novelty and usefulness.

To identify a microorganism that decomposes chitin, we screened from composts on Ishigaki Island at 60°C in an anaerobic environment using a medium containing crystalline chitin as a carbon source. A new genus and new species of chitin-degrading, thermophilic anaerobic bacterium was successfully isolated and identified as *Capillibacterium thermochitinicola* UUS1-1 (Fig. 1). This bacterium is taxonomically positioned in the OPB54 cluster of uncultured bacteria of the phylum *Firmicutes*, a gram-positive bacterium. Its discovery as a bacterium that can be cultivated in the OPB54 cluster followed that of the previously known *Hydrogenispora ethanolica*. Strain UUS1-1 is the first thermophilic anaerobic bacterium that has been confirmed to be able to decompose and assimilate crystalline chitin by producing two types of chitin-degrading enzymes (Fig. 2). From genome analysis, strain UUS1-1 has at least 6 chitin-degrading enzymes and metabolic pathways required for chitin utilization, and it can produce hydrogen directly from chitin. Strain UUS1-1 has been deposited as a reference strain at RIKEN BioResource Center (JCM 33882T) and German Microbial Cell Culture Collection Center (DSM 111537T).

(A. Kosugi, A. Uke, S. Baramée, U. Ungkulpasvich [University of Tsukuba])

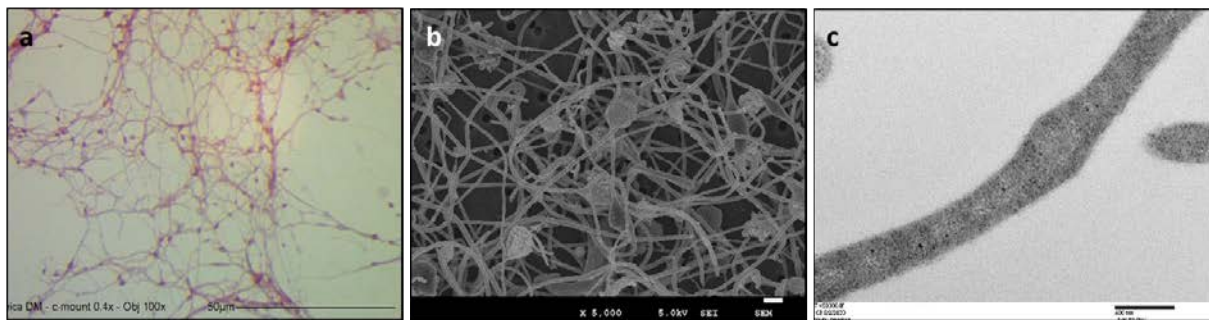


**Fig. 1. Morphological observation of *C. thermochitinicola* UUS1-1**

a: UUS1-1 optical micrograph (black horizontal bar scale at the bottom of the photo is 50  $\mu\text{m}$ ), b: UUS1-1 scanning electron micrograph (white horizontal bar scale at the bottom of the photo is 1.0  $\mu\text{m}$ ), c: transmission electron micrograph (black horizontal bar scale at the bottom of the photo is 0.4  $\mu\text{m}$ ).

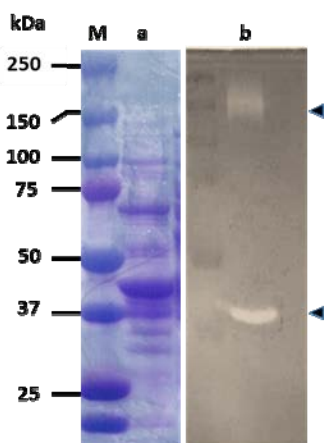


**Fig. 2. Chitin degradation ability by extracellular enzyme of *C. thermochitinicola* UUS1-1**

a: SDS-PAGE of the extracellular enzyme of the isolate UUS1-1, b: Zymogram analysis on chitin degradation activity of the extracellular enzyme prepared from the isolate UUS1-1. ▲: Chitin degradation activity is observed in the molecular weight.

M: Molecular weight marker



## **Initial salinity adjustment effectively prevents histamine accumulation in *padaek*, a Laotian salt-fermented freshwater fish paste**

*Padaek* is a shelf-stable salt-fermented freshwater fish paste popularly used for seasoning various Laotian dishes. Pieces of fish remaining in the fermented product can also be cooked for consumption. Although commercial products are currently available, *padaek* is still made and eaten at home in rural areas to make use of indigenous freshwater fish as an important source of nutrition. In traditional *padaek* production, the fish are washed with water and then mixed with salt and rice bran at a ratio by weight of 3:1:1 to adjust the salinity to around 20%, which is common in *padaek* products in Laos. Halophilic lactic acid bacteria, such as *Tetragenococcus halophilus* and *muriaticus*, are found in the fermented product. According to the producers, *padaek* is considered edible after 2 to 3 months of fermentation, with further fermentation for at least 6 months or more to make it more palatable.

Histamine is an endogenous substance in the human body, playing an important role in modulating diverse physiological functions. It can also accumulate in amino-acid-containing foodstuffs including fermented fish due to bacteria that possess amino acid decarboxylation activity. The intake of an excess of dietary histamine can cause poisoning symptoms such as stomach upset and hives. Histamine levels of 500 to 1,000 ppm in foodstuffs are considered to be potentially hazardous to human health, although the sensitivity to histamine is largely varied between individuals. Research on the histamine level in *padaek* and its accumulation mechanism is needed to develop a strategy for preventing excessive histamine accumulation that could adversely affect nutrition security and human health.

Histamine levels in *padaek* made in rural households negatively correlated with the salinity (Fig. 1). Experimental *padaek* fermentation with initial salinity of 10% and 6.5% exhibited significant histamine accumulation after 2 weeks of fermentation, while no histamine was detected with initial salinity of 18% for 6 months (Fig. 2), indicating that salinity was a critical factor for controlling the risk of histamine accumulation during *padaek* fermentation. Households in the rural village were invited to further test the practicability of salinity adjustment to reduce histamine accumulation in their *padaek*. For that purpose, we prepared a simplified calculation chart (Fig. 3) by referencing a traditional recipe to ensure that the weight ratio of fish, salt, and rice bran was 3:1:1. The participants were instructed on how to use the chart to properly adjust the initial salinity in their *padaek* fermentation. The average salinity and histamine contents of *padaek* produced by the participants after the instruction were significantly higher and lower, respectively, than those in the samples collected in the same village before implementing the salinity management practice (Fig. 4), thus demonstrating the usefulness of salinity adjustment for reducing histamine accumulation in their *padaek*. This producer-friendly approach is recommended for the effective implementation of good manufacturing practice for *padaek* in Laos.

(J. Marui, S. Phouphasouk [Faculty of Agriculture, National University of Laos], S. Boulom [Faculty of Agriculture, National University of Laos])

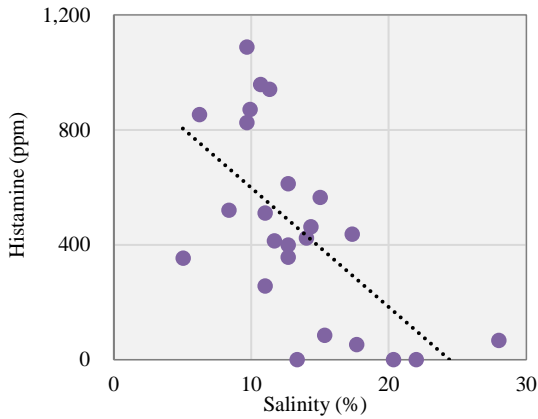


**Fig. 1. Negative correlation between salinity and histamine contents ( $r = 0.633$ ,  $p < 0.01$ ,  $n=24$ ) observed in homemade *padaek* samples collected from rural households**

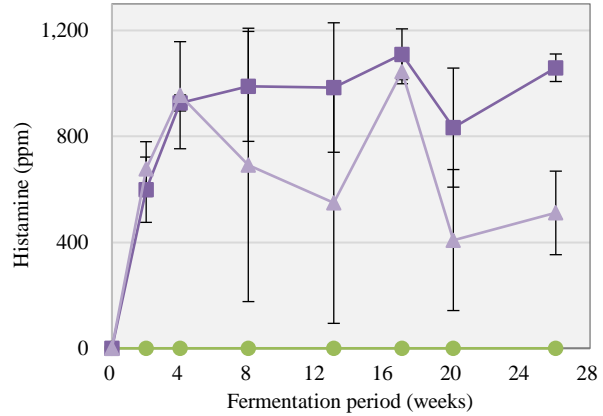


**Fig. 2. Fermentation period-dependent change of histamine contents in experimental *padaek* fermentation under salinities of 18% (●), 10% (■), and 6.5% (▲)**

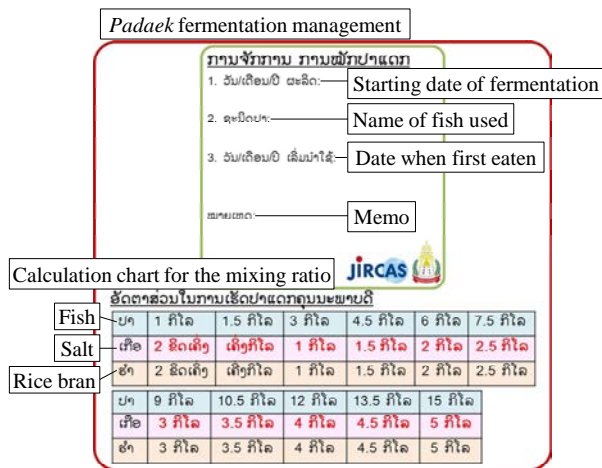


**Fig. 3. Table showing the simplified calculation chart recommended for *padaek* fermentation**

Figure shows English translation of the Lao language used in the table.

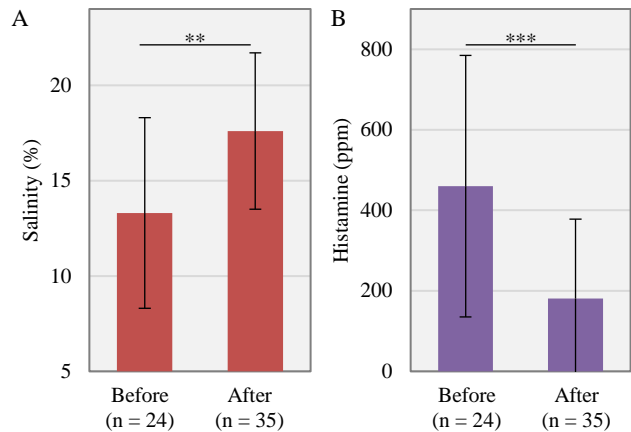


**Fig. 4. Comparisons of average salinity (A) and histamine content (B) of homemade *padaek* samples collected from the village before implementing the salinity management practice (Before) and the samples from the households after being instructed on how to adjust the initial salinity using the simplified calculation chart (After)**

## **Rice and weeds in upland rice fields can be discriminated with good accuracy from a commercial-grade small drone**

Weed control is an important task to improve the productivity of upland rice, which is a major crop in Laos. Aerial images of fields taken with drones are effective tools for early detection of weeds and rapid herbicide treatment, but there is no practical method that can be used in farm fields. Therefore, based on object-based image analysis (OBIA), this study developed a method for discriminating rice and weeds using RGB (Red-Green-Blue) color images of upland rice fields in Laos taken with a commercial-grade small drone.

The experimental results are summarized as follows.

- In an experimental field (furrow 25 cm × 25 cm), a small drone (DJI Phantom 4) was used to capture RGB images at a flight altitude of 20 m (ground resolution 1 cm) 29 days after sowing. HSV (Hue-Saturation-Brightness) and Texture (spatial variance) were calculated from the RGB color image. As training data, the positions of rice, weeds, and soil on the image were collected from the RGB color image by visual interpretation. In OBIA, (1) the images were segmented by similar pixel values using the SLIC (Simple Linear Iterative Clustering) method, (2) statistics were extracted from the segments of classification class (rice, weeds, and soil) in the training data, and (3) the extracted statistical values were used as explanatory variables for random forest classifier.
- OBIA classified rice and weeds, mainly *Asteraceae* and *Legumes*, which dominated the upland rice fields in Laos, with overall accuracy (OA) of 90% or more (Table 1), and provided the spatial distributions (Fig. 2).
- Soil was classified with a recall value of 99.0% even if only the HSV color information was used, but the accuracies of rice and weeds classification could be improved by adding Texture information (Table 1).
- Since the coverage of rice, weeds, and soil classified from the drone changed between 1, 17, and 34 days after weeding (Fig. 3), it is possible to quantitatively grasp the situation in which weeds grow over time after weeding treatment.

Rice and weeds could be rapidly discriminated with practical accuracy by OBIA with a small drone. Farmers can grasp the weed growth in the field at an early stage and use it as basic information for appropriate weed management (herbicide treatment). If this method is applied to field phenotyping, the influence of weeds can be removed from the image without weed removal in the field, and improvement of the accuracy and efficiency for rice growth monitoring can be expected. It should be noted that it is possible to fly at a higher altitude to shoot a wider area in a short time, but the classification accuracy will decrease accordingly, so it is necessary to formulate a flight plan that suits the purpose of use. In addition, the classification accuracy may decrease for weed species with similar morphology, such as grass weeds.

(K. Kawamura, H. Asai, S. Phongchanmaixay [NAFRI, Laos])

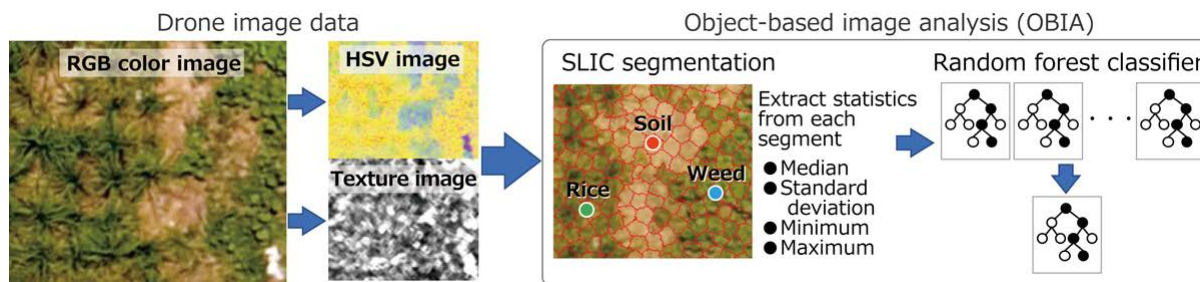


**Fig. 1. Processing flow of object-based image analysis using HSV image and Texture image (spatial variance) calculated from RGB color image of drone**

Extracted statistics from the segments created by the SLIC (Simple Linear Iterative Clustering) method are used as input values for random forest classifier.



**Fig. 2. Spatial distribution map of rice, weed, and soil classified by object-based image analysis of drone images**

Comparison of treatment plots with different days after weeding (1, 17, and 34 days after weeding)

Table 1. Confusion matrix in random forest classification

	True class	Classified as			Recall
		Rice	Weed	Soil	
<b>(a) HSV (OA = 0.901, F-score = 0.900)</b>					
True class	Rice	82	18	0	0.820
	Weed	11	89	0	0.890
	Soil	1	0	99	0.990
Precision		0.872	0.832	1.000	
<b>(b) HSV + Texture (OA = 0.910, F-score = 0.906)</b>					
True class	Rice	83	17	0	0.830
	Weed	9	91	0	0.910
	Soil	1	0	99	0.990
Precision		0.892	0.843	1.000	

OA: overall accuracy

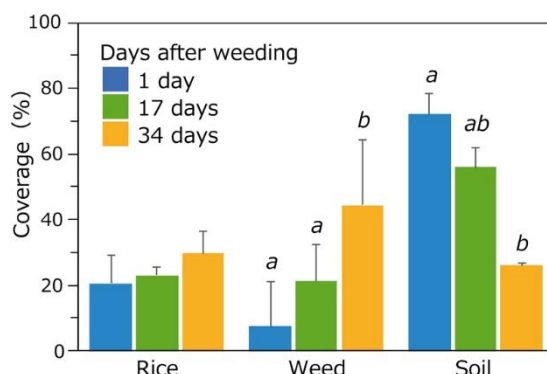


**Fig. 3. Comparison of rice, weed, and soil coverages**

Different letters on the bar indicate significant differences at 5% level (Tukey HSD).

## **Possibility to introduce genomic selection into tree breeding for important timber species distributed in the tropical rainforests of Southeast Asia**

In Southeast Asian rainforests, commonly adopted logging systems allow only trees larger than the regulated cutting limit to be selectively felled, with the next harvest expected after the forests have naturally recovered (35-year rotation in Indonesia). However, poor recovery and a decline in production levels have caused problems in second and further harvesting. Indonesia, which has the largest tropical rainforest in Southeast Asia, is implementing a system that restores productivity by artificial planting after logging, but the seedlings have not been genetically improved. Thus, this research aimed to clarify how genetically improved seedlings greatly contribute to the recovery of tropical rainforests and the improvement of productivity.

In recent years, advances in next-generation sequencing have made it possible to detect genome-wide DNA polymorphisms from a large number of individuals. This technology allows the development of a genomic prediction model that can estimate phenotypes from DNA polymorphisms, which can be used for the selection of superior progenies in the next generation (genomic selection). Conventional forest tree breeding requires a long period of time to evaluate phenotypes due to their longevity, but predicting future phenotypes from DNA polymorphisms at seedling stage can significantly shorten the breeding cycle. Therefore, to restore the rainforest and improve productivity with superior seedlings, we clarified the possibility of genomic selection for dipterocarp species, which are the dominant tree species in the rainforest and provide various ecosystem services including timber production.

Genome-wide DNA polymorphisms (5,900 loci) were obtained from 356 progenies derived from open-pollinated mating of 77 mother trees of *Shorea platyclados*, one of the main dipterocarp timber species, which were planted in a progeny trial at a forest concession area in central Kalimantan. Linkage disequilibrium over long physical distances showed that the progenies were suitable for genome-wide association studies (GWAS) and genomic predictions. GWAS revealed that a locus showed significant association with tree height before thinning (8th year), but did not exhibit significant association with tree height after thinning (11th year), trunk diameter, tree shape, and wood density, which suggest that these traits are regulated by many weakly effective genes. Selection of informative loci based on GWAS improved genome heritability, which represented that phenotypic variance was well explained by the genotype of the selective loci (Table 1). Furthermore, the genomic heritability of growth-related traits is higher than that of tree shapes and wood density. Therefore, genomic selection is particularly effective for breeding fast-growing individuals.

We identified that deep learning and increasing the numbers of analyzed individuals and loci contribute to improving the accuracy of the genomic prediction model. Using the developed genome prediction model, selection of seedlings for growth-related traits will lead to a significant shortening of the breeding cycle. However, our results suggest that these traits are regulated by many weakly regulated genes, hence are not suitable for marker-assisted selection. (N. Tani, R. Suwa, Sawitri [Universitas Gadjah Mada (UGM)], M. Na'iem [UGM], Widiyatno [UGM], S. Indrioko [UGM], K. Uchiyama [FFPRI], Y. Tsumura [University of Tsukuba])

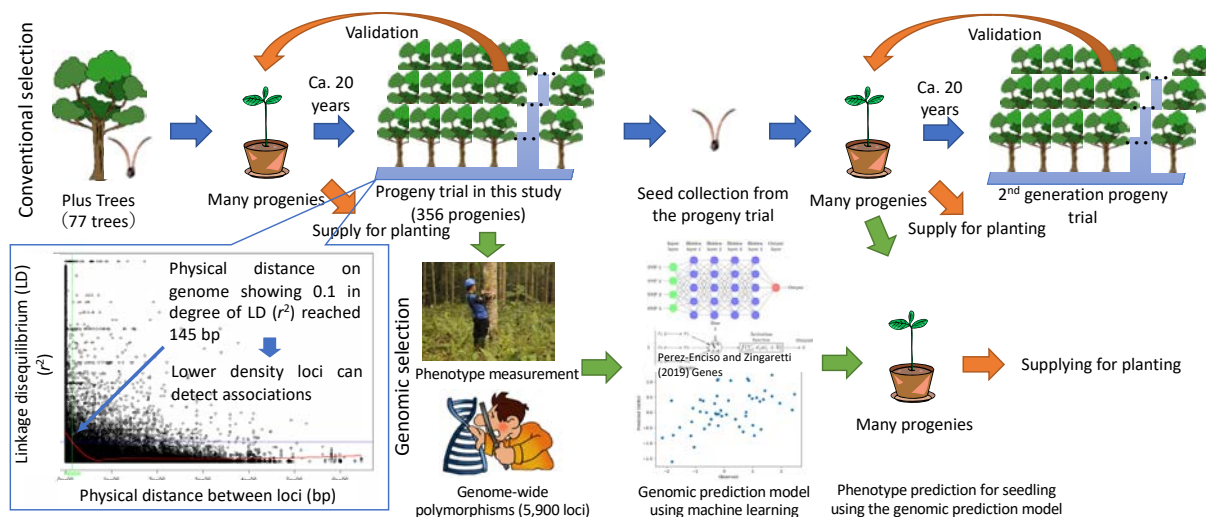


**Fig. 1. Genetic characteristics of the progeny trial in this study and genomic selection**  
 Conventional selection requires about 20 years for validation. The genomic prediction model can shorten this process, which in turn can shorten the breeding cycle.

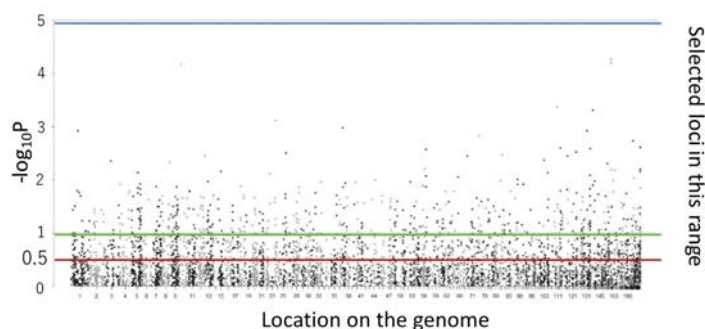


**Fig 2. Manhattan plot showing association between tree height after thinning and genotype of each loci**

GWAS on all measured traits showed no significant association except for a significant locus on tree height before thinning.

**Table 1. Genomic heritability estimated from genotypes**

	Genomic heritability All loci	Genomic heritability Selected loci
Tree height after thinning (11 years)	0.313	0.573
Trunk diameter after thinning	0.292	0.615
Branch angle	0.190	0.342
Wood density	0.263	0.516
Wood swiftness	0.252	0.473

Genomic heritabilities on growth (tree height and trunk diameter) were improved when the loci were selected using a  $-\log_{10}P$  value threshold of 0.5 (red line in Fig. 2), which indicated that there are many associated genes with weak effect.



## Temperature-regulated leaf production in the family Dipterocarpaceae

Dipterocarpaceae is a dominant tree family in Southeast Asia. This family consists of more than 500 species, many of which are important timber trees. To achieve sustainable timber production of dipterocarp species, a stable supply of planting materials is required. However, dipterocarp species flower at irregular intervals from three to ten years, which leads to difficulties in collecting seeds and providing good planting materials. To overcome the shortage of planting materials, we studied the regulation of growth in dipterocarps. Understanding their growth regulation helps to supply dipterocarp saplings by controlling their growth.

For this purpose, we focused on leaf production as an indicator of plant growth. We developed an observation system using time-lapse digital cameras and monitored daily leaf production by two dipterocarp species, *Shorea leprosula* and *Neobalanocarpus heimii* (Fig. 1). To exclude the effect of rainfall variations on leaf production, we covered the observation system with transparent plastic sheets and installed it in the nursery of Forest Research Institute Malaysia (FRIM). The observation showed that leaf production by dipterocarp saplings fluctuated without variation in rainfall (Fig. 2). This suggests that the timing of leaf production cannot be explained by the rainfall pattern. Instead, we found similarities in leaf production and temperature patterns (Fig. 2). Thus, to test the effect of temperature on the timing of leaf production, we applied Convergent Cross Mapping (CCM) to the observation result. CCM is a mathematical framework to analyze causal relationships between time-series data. The CCM analysis showed that estimation skill from leaf to temperature data (cross-map skill: 0.20) was higher than that of surrogate data (cross-map skill: 0.18), suggesting a causal relationship between temperature and leaf production. The growth chamber experiments showed that leaf production was significantly increased by small increments (5°C) in daytime or nighttime temperature from baseline temperature (daytime: 27°C, nighttime: 24°C) (Fig. 3). These results indicate that temperature is a regulator of leaf production.

Because our results showed that temperature affects the growth of dipterocarp saplings, if we grow the saplings in the nurseries under different temperature regimes, their growth would be varied. Thus, the establishment of multiple nurseries in different temperature conditions would diversify the supply time of good planting materials, which will contribute to a stable supply of planting materials and sustainable timber production of dipterocarps.

(M. J. Kobayashi, N. Tani, K. K. S. Ng [Forest Research Institute Malaysia], S. L. Lee [Forest Research Institute Malaysia], N. Muhammad [Forest Research Institute Malaysia])



**Fig. 1. Leaf production observation system using time-lapse digital cameras**

To exclude the effect of rainfall variations on leaf production, the observation system was covered with transparent plastic sheets.

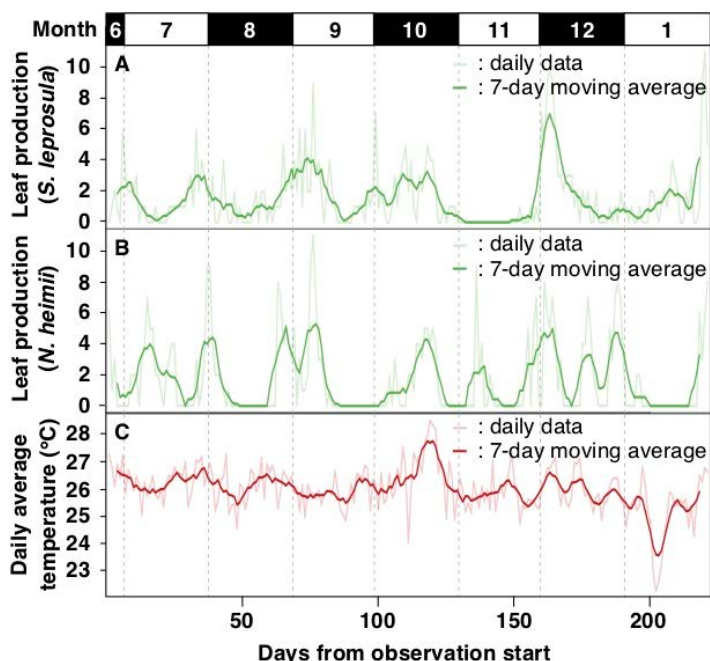


**Fig. 2. Daily leaf production and temperature data obtained by the observation system** (A) No. of produced leaves by *Shorea leprosula*, (B) No. of produced leaves by *Neobalanocarpus heimii*, and (C) Daily average temperature. The data were obtained from June 2017 to January 2018.

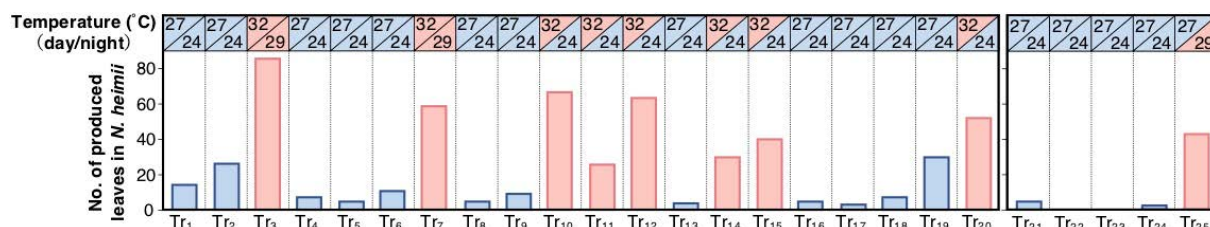


**Fig. 3. Relationship between temperature and leaf production in the growth chamber**  
 The growth chamber experiment was conducted using 50 individuals of *N. heimii*. Tr<sub>x</sub> indicates ~3-week temperature treatment. The experiment from Tr<sub>21</sub> was conducted as a separate experiment. The temperatures in upper and lower triangles indicate daytime (7 AM to 7 PM) and nighttime (7 PM to 7 AM) temperatures, respectively.

## Development of models for estimating mangrove aboveground biomass at regional scale

Mangroves are unique ecosystems developed in brackish water areas where plants are exposed to physiologically stressful conditions such as high-salinity and anaerobic environments (Fig. 1). Recently, the huge amount of carbon stocks in mangroves have been the focus of studies due to its relevance to climate change, and mangroves have been recognized as very important for storage of blue carbon, which is carbon sequestered in marine ecosystems. To evaluate the ability of mangroves to sequester carbon, biomass estimation over wide regions is essential. In general, biomass estimation is conducted with remote sensing techniques, such as the airborne Light Detection and Ranging (LiDAR) system, to measure average canopy height, which is then converted to biomass using models developed by field researchers. However, models for converting canopy height to biomass were scarce for mangroves in Southeast Asian regions. Therefore, we developed a mangrove model for Asian regions based on field studies conducted at mangroves in the Philippines, Indonesia, and Japan.

Our results confirmed that the relationships of aboveground biomass (AGB) to average canopy height for upper-canopy trees showed apparent differences between terrestrial tropical forests and mangroves, where mangroves showed approximately four times higher AGB specific to the canopy height than that of terrestrial forests (Fig. 2). On the other hand, the cumulative basal area  $BA$  was approximately two times higher in mangroves than in terrestrial forests (Fig. 3). Thus, the high AGB specific to canopy height can be partly explained by their unique characteristics having higher tree density of thick stem trees. Finally, we successfully proposed a common mangrove model for Asian regions as  $Y = 2.25X^{1.81}$  ( $R^2 = 0.66$ ), where  $Y$  and  $X$  are AGB in  $\text{Mg ha}^{-1}$  and the average canopy height in m, respectively.

The developed model for estimating AGB with canopy height can be applied for evaluating the carbon stock of mangroves in Asian regions with remote sensing techniques. It should be noted, however, that the developed model cannot be applied to open-canopy mangroves. Furthermore, the developed model tends to underestimate AGB for large forests whose  $\text{AGB} > \text{ca. } 400 \text{ Mg t ha}^{-1}$ .

*(R. Suwa, R. Rollon · G. M. G. Albano · A. C. Blanco [University of the Philippines], S. Sharma [Malaya University], M. Yoshikai, K. Nadaoka [Tokyo Institute of Technology], K. Ono [Forestry and Forest Products Research Institute, Japan], N.S. Adi · R. N. A. Ati · M. A. Kusumaningtyas · T. L. Kepel [Ministry of Marine Affairs and Fisheries, Indonesia], R. J. Maliao, Y. H. Primavera-Tirol [Aklan State University, Philippines])*



**Fig. 1. Mangroves inundated with brackish water**  
Photo taken at a study site in the Philippines

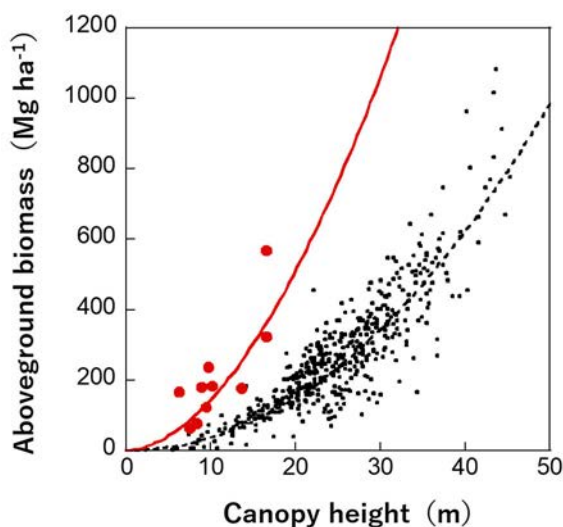


**Fig. 2 Relationships of aboveground biomass to canopy height**

Red dots and black dots mean mangroves and terrestrial forests, respectively. The solid red line and dashed black line mean regression models for mangroves (the present study) and terrestrial forests (Saatchi et al. 2011 in *PNAS*).

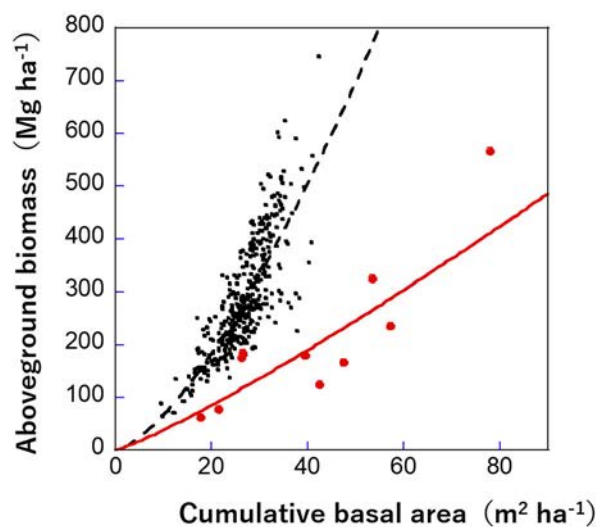


**Fig. 3. Relationships of aboveground biomass to cumulative basal area**

Red dots and black dots mean mangroves and terrestrial forests, respectively. The solid red line and dashed black line mean regression models for mangroves (the present study) and terrestrial forests (Mitchard et al. 2014 in *Global Ecol. Biogeogr.*).

### **Use of a filamentous green alga (*Chaetomorpha* sp.) and microsnail (*Stenothyra* sp.) as feed at an early stage of intensive aquaculture promotes profitability of giant tiger prawn**

Shrimp is a major export item; hence, high Penaeidae shrimp production in intensive aquaculture systems contribute to the economic development of shrimp-producing countries. However, decreasing shrimp productivity and profitability have been reported owing to a deterioration in artificial feed quality and the soaring prices of artificial feed. Following a series of research activities on Penaeidae aquaculture in Southeast Asian countries, JIRCAS was able to develop a simple, low-cost, and sustainable technique to boost productivity, feed efficiency, and profitability of the giant tiger prawn. The aim of this study was to verify the profitability of giant tiger prawn grown in an innovative aquaculture system, in which a filamentous green alga (*Chaetomorpha* sp.) and microsnail (*Stenothyra* sp.) are cultured together during early stage and freely consumed as supplementary live feeds in intensive aquaculture ponds.

Post-larvae (mean wet weight: 2 mg, mean total length: 9 mm) of giant tiger prawn were released and cultured at a density of approximately 33 individuals m<sup>-2</sup> in outdoor concrete ponds (9 m × 9 m × 1.2 m) at King Mongkut's Institute of Technology Ladkrabang (KMITL), Thailand, under either control (fed only artificial feed,  $n = 3$ ) or experimental (fed artificial feed and benthic organisms,  $n = 3$ ) conditions (Fig. 1) until they reached marketable size (15 weeks) (Fig. 2, Table 1). Compared with the control group of giant tiger prawn, the experimental group significantly improved in terms of productivity (33%), feed efficiency (12%), and profitability (46%) when provided ~8% green alga to total feed consumption and ~2% microsnail to total feed consumption at an early stage of culture. The individual shrimp weight became significantly higher in the experimental treatment ponds (median: 1.12 g, mean: 1.44 g) than those in the control ponds (median: 0.70 g, mean: 0.80 g) at week 4. The technique developed in this study will help enhance productivity, feed efficiency, and profitability in intensive giant tiger prawn aquaculture operations.

From these results, it is expected that this can be applied to Penaeidae intensive aquaculture management systems other than those for giant tiger prawn. Both green alga, *Chaetomorpha* sp., and microsnail, *Stenothyra* sp., were all consumed within 1–2 months due to active grazing by the giant tiger prawn. These two benthic organisms could be propagated for longer periods in shrimp culture ponds for higher productivity, feed efficiency, and profitability.

(I. Tsutsui, D. Aue-umneoy [King Mongkut's Institute of Technology Ladkrabang])

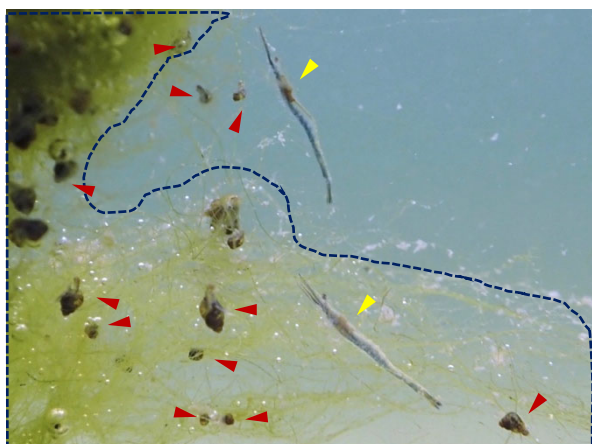


**Fig. 1.** Post-larvae (Total length: ~9 mm, yellow arrows), *Chaetomorpha* sp. (area within dark blue broken line) and *Stenothyra* sp. (red arrows)



**Fig. 2.** Sorting operation at a shrimp broker company for giant tiger prawn produced from this study

**Table 1. Results of the 15-week giant tiger prawn aquaculture experiment in a concrete pond at KMITL**

	Control (n = 3)	Experimental treatment (n = 3)
<b>Growth and productivity</b>		
Final mean individual shrimp weight (g WW)	16.0 ± 0.61	18.2 ± 1.07 *
Total shrimp production (kg WW)	33.0 ± 1.8	43.9 ± 0.5 *
<b>Feed intake and efficiency</b>		
Apparent <i>Chaetomorpha</i> intake (kg WW)	—	6.81 ± 1.45
Apparent <i>Stenothyra</i> intake (kg WW)	—	1.96 ± 0.05
Apparent artificial feed intake (kg WW)	61.0 ± 3.2	72.0 ± 3.8 *
Feed efficiency (%)	54.1 ± 1.8	61.1 ± 4.0 *
<b>Costs and profitability</b>		
Artificial shrimp feed costs (USD) (a)	83.55 ± 4.45	98.59 ± 5.24 *
Miscellaneous costs (USD) (b)	—	12.11 ± 0.00
Shrimp sales (USD) (c)	155.73 ± 10.27	215.97 ± 4.37 *
Balance between shrimp sales and costs (USD) (c-a-b)	72.18 ± 7.55	105.27 ± 3.02 *

Values are shown as mean ± standard deviation from triplicate data.

Superscript labels within the same row indicate significant difference (t-test,  $p < 0.05$ ). Feed efficiency (%) is calculated as  $100 \times \text{weight gain} /$

Feed amount intake. Common costs between mono-culture and co-culture

such as water charges, electric fees, labor, culture materials, etc. are

omitted in order to easily compare the profitability results.

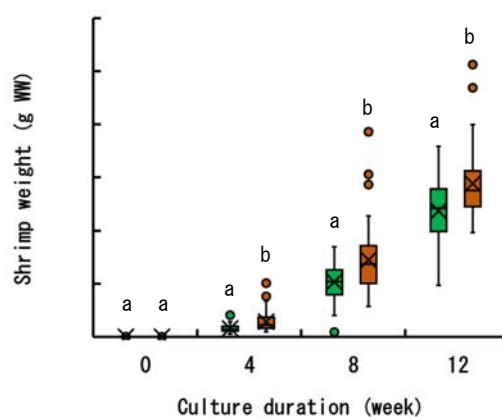


**Fig. 3. Changes in wet weight of giant tiger prawn under control (green) and treatment (orange) conditions**

Different lowercase letters within the same sampling week indicate a significant difference between treatments (Mann-Whitney U-test,  $p < 0.05$ , adjusted via the Bonferroni correction for multiplicity)



## Development of conventional biological indices for evaluation and management of blood cockle fishing/aquaculture grounds

The blood cockle, *Tegillarca granosa* (Fig. 1), is an especially important fisheries resource for Southeast Asia. It is rich in minerals and vitamins, and is an indispensable ingredient in traditional dishes to improve nutritional balance of the local people. These days, production of blood cockle in Southeast Asia is seriously decreasing because of environmental deterioration in the coastal areas where their habitats are. Therefore, appropriate management of the fishing and aquaculture grounds as well as technical measures to recover the bivalve resources are required. For that purpose, easy and economical monitoring techniques are needed to evaluate long- and short- term changes in the bivalve's living environment.

To monitor the condition of the fishing/aquaculture grounds of blood cockle continuously, we developed simple biological indices which can be obtained easily by local fishers. We modified the conventional sharpness index in bivalve shell profiles (shell width / shell length) and applied it to blood cockle to examine its growth conditions. The adjusted sharpness index was deduced from the allometric equation to remove size dependency in the conventional sharpness index (Fig. 2A, Eq. 1). It could be used for blood cockle samples of mixed sizes to detect growth difference between groups from different origins (Fig. 3) to evaluate habitat suitability. For example, a trend in increasing adjusted sharpness index in the same fishing ground suggests environmental deterioration is in progress, causing the growing of the inhabiting blood cockle worse. Thus, we may recommend changing the location of fishing /aquaculture grounds. On the other hand, we examined a new method to estimate the condition factor (soft tissue weight / total wet weight) quickly (Fig. 2B, Eq. 2). We found that shell width can be used as a good estimator of shell weight. The soft tissue weight can be calculated as total wet weight of the bivalve minus total shell weight. In this manner, the condition factor could be calculated from total wet weight and shell width without opening the cockles. A trend in decreasing the condition factor suggests the soft tissue of the blood cockle is getting thinner. Thus, we may recommend harvesting the cockles sooner.

The adjusted sharpness index and the estimated condition factor would provide powerful tools to monitor long- and short-term growth conditions of blood cockles, and to evaluate the condition of its fishing/aquaculture grounds indirectly. The developed biological indices would provide fisheries authorities scientific evidence to make recommendations for blood cockle fishery management. The developed indices can be calculated easily by measuring only three body size variables — length, width, and total weight — using simple tools such as calipers and weighing scales, therefore even fishers can utilize them. JIRCAS has worked together with our counterpart in Malaysia to construct a data collection and monitoring scheme for the management of blood cockle fishing/aquaculture grounds (Fig. 4).

*(H. Saito [Fisheries Technology Institute],  
H. W. Teoh [China-ASEAN College of Marine Sciences, Xiamen University, Malaysia])*



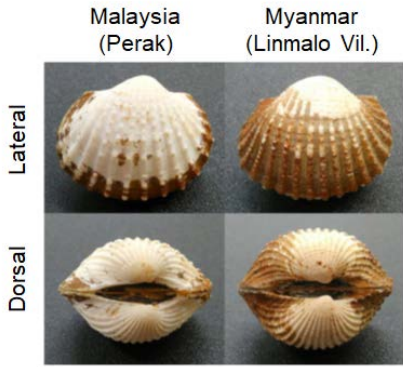
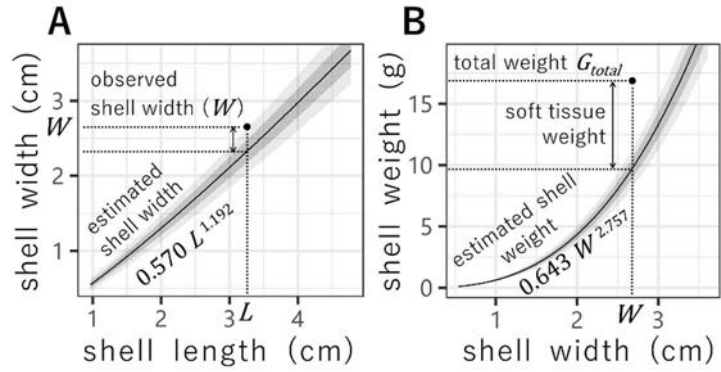


**Fig. 1. Blood cockles, *Tegillarca granosa*, collected from Perak, Malaysia (left) and from Linmalo Village, Myanmar (right)**



$$SI_{adj} = \frac{W - 0.570L^{1.192}}{L} \quad \dots \text{Eq. 1}$$

$$CF = \frac{G_{total} - 0.643W^{2.757}}{G_{total}} \quad \dots \text{Eq. 2}$$

$SI_{adj}$ : Adjusted sharpness index,  $W$ : Shell width (cm),  
 $L$ : Shell length (cm),  $CF$ : Condition factor,  $G_{total}$ : Total wet weight

**Fig 2. Scatter plots to estimate equations for the adjusted sharpness index (A) and the condition factor**  
 Each plot was superimposed with the allometry curve (black line) and 68% (light grey) and 95% (grey) prediction intervals.

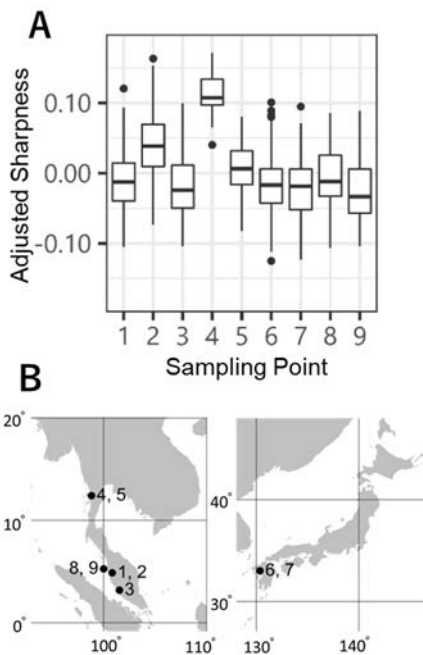


**Fig 3. Adjusted sharpness indices of blood cockles (A) from sampling points (B)**

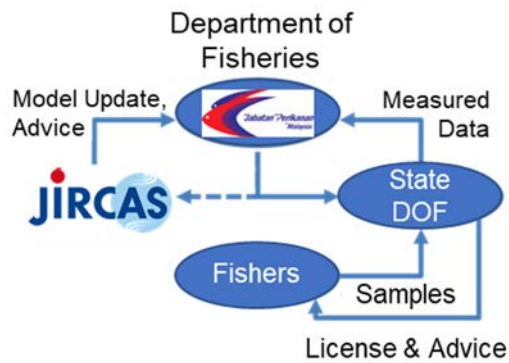


**Fig 4. Schematic model to monitor and manage blood cockle fishing/aquaculture grounds in Malaysia**